energies

MDPI

Article

Assessment of Power-Law Viscosity Models for Binary Lubricating Oil–EN 590 B7 Diesel Mixtures as a Tool for Evaluating Diesel Oil Dilution

Magdalena Szmukała [1], Iwona Michalska-Pożoga [2], Marcin Szczepanek [3,*] and Leszek Chybowski [4,*]

[1] Centre for Research on Fuels, Working Fluids and Environmental Protection, Faculty of Marine Engineering, Maritime University of Szczecin, ul. Willowa 2, 71-650 Szczecin, Poland; m.szmukala@pm.szczecin.pl
[2] Department of Processes and Equipment of the Food Industry, Faculty of Mechanical and Power Engineering, Koszalin University of Technology, ul. Sniadeckich 2, 75-453 Koszalin, Poland; iwona.michalska-pozoga@tu.koszalin.pl
[3] Department of Power Engineering, Faculty of Marine Engineering, Maritime University of Szczecin, ul. Willowa 2, 71-650 Szczecin, Poland
[4] Department of Marine Propulsion Plants, Faculty of Marine Engineering, Maritime University of Szczecin, ul. Willowa 2, 71-650 Szczecin, Poland
* Correspondence: m.szczepanek@pm.szczecin.pl (M.S.); l.chybowski@pm.szczecin.pl (L.C.)

Abstract

Diesel oil dilution of lubricating oil is an important phenomenon affecting its viscosity and, consequently, the lubrication conditions and operational reliability of internal combustion engines. The viscosity of a lubricating oil–biodiesel oil mixture can therefore be used as a parameter for assessing the degree of fuel dilution. This study evaluates the applicability of selected power-law viscosity models for describing binary mixtures of lubricating oil and EN 590 diesel oil containing 7% bio-component (fatty acid methyl esters) by mass. Two lubricating oils, SAE 30 and SAE 40 grades, were investigated at diesel oil concentrations of 0, 1, 2, 10, 20, 50 and 100% by mass over a temperature range of 40–100 °C. The experimental results were compared with four power-law models, the linear, Kendall–Monroe, Koval and Bingham models, with the Arrhenius and REFUTAS models included as reference models. The novelty of the study lies in the systematic comparison of the power-law models over a broad range of temperature and dilution levels and their performance assessment against the Arrhenius and REFUTAS models. The relative error between calculated and experimental viscosities was determined for all investigated conditions. The linear model showed the lowest accuracy, followed by the Kendall–Monroe and Bingham models. The Koval model demonstrated the highest accuracy among the power-law models, with a maximum relative error of less than 9%, outperforming the Arrhenius model and showing accuracy comparable to that of the REFUTAS model. The results also show that model suitability depends on mixture composition and temperature, and that the distribution of prediction errors should be considered alongside their magnitude. The Koval model may therefore provide a simple and sufficiently accurate alternative for describing lubricating oil–diesel oil mixtures and assessing diesel oil dilution.

Keywords: lubricating oil dilution with fuel; lubricating oil; diesel oil; power-law viscosity model; REFUTAS; Arrhenius equation; viscosity mixing model

Check for updates

Academic Editor: Diego Luna

Received: 9 September 2026
Revised: 30 September 2026
Accepted: 2 October 2026
Published: 7 October 2026

Copyright: © 2026 by the authors. Licensee MDPI, Basel, Switzerland. This article is an open access article distributed under the terms and conditions of the Creative Commons Attribution (CC BY) license.

1. Introduction

The viscosity of lubricating oil is one of the fundamental parameters determining the quality of the lubrication process in internal combustion engines. Its value affects the formation and stability of the lubricating film, friction losses, heat transfer and wear of cooperating surfaces [1,2]. During engine operation, however, the viscosity of the lubricant may change as a result of contamination and degradation processes. One of the particularly important phenomena is the dilution of lubricating oil by diesel oil, which can lead to a significant reduction in viscosity and, consequently, deterioration of the lubrication conditions [3,4]. In this study, diesel oil (DO) containing 7% fatty acid methyl esters (FAME) by mass as a bio-component was used as the diluent of the lubricating oil, representing a commonly used type of diesel fuel currently marketed in the European Union.

Diesel oil dilution may occur as a result of incomplete combustion, diesel oil leakage past the piston rings, injector malfunctions, excessive diesel oil delivery, leakage from fuel pumps, or improperly functioning fuel leakage drainage systems, as well as operating conditions favouring the condensation of diesel oil on cylinder liner surfaces [5–8]. The severity of this phenomenon depends on the engine design, diesel oil properties, operating conditions and technical condition of the diesel oil injection and combustion systems [9–11]. Since excessive diesel oil dilution may contribute to increased wear and other lubrication-related failures [12,13], the possibility of determining the diesel oil content in lubricating oil is of considerable practical importance [14,15].

Viscosity measurements provide a relatively simple basis for assessing diesel oil dilution. The relationship between the viscosity of a binary mixture and the viscosities and concentrations of its components can be described using various mathematical models. Among the relatively simple approaches to predicting mixture viscosity are power-law models, which relate the viscosity of a mixture to those of its components and their respective mass fractions [16]. These include the linear mixing model [17,18], Kendall and Monroe model [17], Koval model [19], and Bingham model [20,21].

The investigated viscosity models differ in the mathematical formulation used to describe the relationship between the viscosities of the mixture components and their mass fractions [16]. The linear model represents the simplest case of the general power-law relationship, obtained for an exponent of k = 1. The Kendall–Monroe model is also a power-law formulation, with k = 1/3, whereas the Koval and Bingham models use negative exponents of k = −1/4 and k = −1, respectively [16]. Thus, these four models represent different forms of the same general power-law relationship and allow the effect of the exponent on the prediction of mixture viscosity to be investigated. The Arrhenius model provides a different formulation based on the logarithmic combination of the component viscosities and their mass fractions. In contrast, the REFUTAS model is based on kinematic viscosity and the Viscosity Blending Index (*VBI*), with the viscosity of the mixture determined from the mass-weighted *VBI* values of its components. The Arrhenius and REFUTAS models were therefore included as reference formulations, allowing the predictive performance of the simpler power-law models to be assessed against models based on different mathematical approaches.

The mathematical simplicity of power-law models is an important advantage, particularly when the models are intended for practical or computational applications [16,18,22]. Depending on the specific formulation, the contribution of individual components is expressed using composition variables such as mole, mass, or volume fraction [18,22]. In the present study, mass fractions were used for the power-law models, consistent with the formulation adopted for the Arrhenius [23] and REFUTAS [24,25] models considered to or comparison. The use of mass fractions is also particularly relevant to the practical assessment of diesel oil dilution, as fuel content in lubricating oil is commonly expressed

on a mass basis [16]. It provides a direct measure of the amount of diesel oil present in the lubricant and allows the investigated mixtures to be prepared and characterised directly on a mass basis. Furthermore, using mass fractions avoids the need to convert between mass and volume fractions using component densities, which would introduce an additional temperature-dependent factor because the densities of both lubricating oil and diesel oil vary with temperature. Thus, expressing the component proportions on a mass basis provides a consistent and practically relevant framework for comparing all the investigated models over the full temperature and concentration ranges.

In addition to the power-law models, two non-power-law approaches were considered. The Arrhenius model is a commonly used relationship for describing the viscosity of binary mixtures, while the REFUTAS model provides a more advanced approach for predicting the kinematic viscosity of diesel oil blends [26]. Both models are formulated using mass fractions and can also be expressed in inverse form, allowing the concentration of one component to be estimated from the measured viscosity of the mixture. This makes them particularly relevant as reference models for assessing the accuracy of the simpler power-law formulations in the context of diesel oil dilution of lubricating oil.

Previous investigations have demonstrated that the inverse Arrhenius relationship can provide a satisfactory estimation of diesel oil concentration in lubricating oil [27], whereas the REFUTAS-based approach called SATUFER [26] can provide substantially higher accuracy [28]. Further improvement can be achieved by optimisation of the parameters of the REFUTAS relationship. These results raise an important question concerning the suitability of simpler power-law relationships. If a power-law model provides a sufficiently accurate description of the actual viscosity of an oil–diesel oil mixture, its mathematical simplicity may make it attractive for practical applications, including the development of methods for estimating diesel oil dilution.

The objective of this study was therefore to assess the ability of selected power-law viscosity models to reproduce the experimentally measured dynamic viscosity of binary lubricating oil–diesel oil mixtures. Two lubricating oils, SAE 30 and SAE 40, were investigated at seven different diesel oil concentrations in lubricating oil–diesel oil mixtures. Measurements were performed at temperatures of 40, 50, 60, 70, 80, 90 and 100 °C. The experimentally determined viscosities were compared with values calculated using the linear, Kendall–Monroe, Koval and Bingham models. The Arrhenius and REFUTAS models were included as reference formulations, owing to their previous application in the inverse determination of diesel oil concentration in lubricating oil.

The model performance was assessed using the relative error between calculated and experimentally measured dynamic viscosity. The error was analysed over the complete temperature–concentration domain and presented using three-dimensional plots. The root mean square relative error (*RMSRE*), the maximum relative error (*MRE*), and the coefficient of determination (R^2) values were used to provide complementary quantitative measures of model performance. This approach makes it possible not only to determine the overall accuracy of each model but also to identify systematic variations in model performance associated with temperature, oil grade and diesel oil concentration. Particular attention was paid to determining whether the simpler power-law models can achieve an accuracy comparable with the more advanced non-power-law formulations and, consequently, whether they have potential for use in applications related to the assessment of diesel oil dilution in lubricating oils.

The novelty of the present study lies in the systematic evaluation of four power-law viscosity models with different exponent values for lubricating oil–diesel oil mixtures and their direct comparison with the Arrhenius and REFUTAS models over a broad range of temperatures and diesel oil concentrations. In contrast to previous studies focused

primarily on the inverse estimation of diesel oil concentration from measured viscosity, the present work evaluates the ability of the models to reproduce experimentally measured mixture viscosity and examines the distribution of prediction errors across the temperature–concentration domain. This approach makes it possible to identify the most suitable power-law formulation for further investigation in the assessment of diesel oil dilution of lubricating oils.

2. Materials and Methods

2.1. Materials Used in the Experimental Study

The experimental study was conducted using Orlen Efecta Diesel Bio fuel (EN 590 B7 diesel oil) [29], which complies with the requirements for liquid fuels specified in ZN-ORLEN-5:2019 [30]. Based on the measured physicochemical properties, the fuel also met the requirements for DMX-category marine distillate fuel specified in 8217:2024 [31]. The lubricating oils selected for the study were single-grade oils of SAE 30 and SAE 40 viscosity grades, representative of lubricants commonly used in marine engines. The oils were supplied as Agip/Eni Cladium 120 CD/CF (Series III). Selected rheological properties of the fuels and lubricants used in the experiments are summarized in Table 1.

Table 1. Selected rheological properties determined for the diesel fuel and lubricating oils used in the experimental study.

Parameter	**Description**		
Oil type	Diesel oil	Lubricating oil	Lubricating oil
Manufacturer and oil designation	Orlen Efecta Diesel Bio CN27102011D	Agip Cladium 120 SAE 30 CD/CF	Agip/Eni Cladium 120 SAE 40 CD/CF
SAE viscosity grade	N/A	SAE 30	SAE 40
Measured density at 15 °C ρ_{15} [kg/m^3] (PN-EN ISO 12185:2024-08 [32])	835.81 ± 0.36	898.29 ± 0.38	898.44 ± 0.38
Calculated temperature coefficient of density ε [kg/(m^3·°C)]	0.706 ± 0.009	0.622 ± 0.009	0.614 ± 0.009
Measured kinematic viscosity at 40 °C ν_{40} [mm^2/s] (PN-EN ISO 3104:2024-01 [33])	2.897 ± 0.033	105.010 ± 0.829	159.900 ± 1.257
Measured kinematic viscosity at100 °C ν_{100} [mm^2/s] (PN-EN ISO 3104:2024-01 [33])	1.232 ± 0.010	11.720 ± 0.068	15.210 ± 0.087
Calculated dynamic viscosity at 40 °C η_{40} [mPa·s]	2.370 ± 0.028	92.690 ± 0.733	141.190 ± 1.111
Calculated dynamic viscosity at100 °C η_{40} [mPa·s]	0.960 ± 0.009	9.91 ± 0.058	12.87 ± 0.074
Viscosity Index *VI* [–] (ASTM D 2270-10(2024) [34])	≥259	99	95
Pour point t_{PP} [°C]	−30 ± 3	−18 ± 2	−15 ± 2

The lubricating oils investigated in this study are formulated for use in naturally aspirated and highly turbocharged diesel engines employed in marine, traction, and industrial applications. Their additive packages are designed to support reliable operation in circulating lubrication systems, including engines operating on both light distillate fuels and lower-quality fuels, such as residual marine fuels and fuels with elevated sulfur content [35,36]. This formulation provides the required protection and supports efficient engine operation under a broad range of fuel conditions. The oils comply with the proprietary specifications of several marine and industrial engine manufacturers, including Deutz MWM, Dorman Diesel, Fincantieri—Divisione Grandi Motori, Isotta Fraschini, MAN B&W, Mirrlees, MTU Marine, New Sulzer Diesel, Nohab, S.E.M.T.–Pielstick, SKL, VM, and Wärtsilä. The experimental design adopted in this study is presented in Table 2.

Table 2. Experimental design for the viscosity measurements.

Lubricating Oil	Diesel Oil Content C [% m/m]	Measurement Temperatures t [°C]	Measured Quantities	Calculated Quantity
SAE 30	0, 1, 2, 5, 10, 20, 50	40, 50, 60, 70, 80, 90, 100	Kinematic viscosity ν, density ρ	Dynamic viscosity η
SAE 40	0, 1, 2, 5, 10, 20, 50	40, 50, 60, 70, 80, 90, 100	Kinematic viscosity ν, density ρ	Dynamic viscosity η

Two lubricating oils, SAE 30 and SAE 40, were investigated at seven diesel oil concentrations: 0, 1, 2, 5, 10, 20, 50 and 100% by mass. A higher number of measurement points was used for diesel oil concentrations of 0–10% w/w, which corresponds to concentrations observed under practical operating conditions, whereas higher concentrations were included to maintain consistency with the authors' previous publications and to enable a comprehensive evaluation of the investigated models over the full composition range [37]. Sample preparation was performed using a RADWAG WPs 510/C/2 precision laboratory balance (Radom, Poland), with a readability (d) of 0.001 g. According to the balance calibration certificate, the maximum permissible indication error (δ) was 0.002 g, as determined for a 400 g reference mass. All samples prepared for the experimental study had a nominal total mass of 200 g [37].

The LO–DO mixtures were prepared gravimetrically to obtain the required mass fraction of diesel oil (DO) in lubricating oil (LO). First, a clean glass container was placed on the balance and tared. The required mass of LO (m_1) was then transferred into the container using a precision laboratory pipette. After re-taring the balance, the required amount of DO (m_2) was added in the same manner. The resulting mixture was subsequently homogenized using a magnetic stirrer for 15 min.

Before each measurement, the repeatability of the balance readings was verified using a reference mass.

The Type B standard uncertainty associated with the determined DO mass fraction was evaluated based on the uncertainty of the gravimetric measurements, following the principles specified in the Guide to the Expression of Uncertainty in Measurement (JCGM 100:2008—GUM 1995 with minor corrections) [38]. The evaluation accounted for the balance readability, the indication error and its associated uncertainty given in the calibration certificate, as well as the repeatability of the balance readings. For each component, the mass used in the preparation of the mixture was determined from the difference between the liquid mass reading and the corresponding tare value. The uncertainty of the total mixture mass was then calculated by combining the relevant uncertainty components. The resulting standard uncertainty of the measured mass (u_m) was 0.0023 g.

The detailed equations used to determine the standard uncertainty of the mass fraction, including the corresponding sensitivity coefficients and uncertainty propagation procedure, are provided in publication [39].

The calculated Type B standard uncertainty, $u_B(C)$, was 0.026% for a DO mass fraction of 1%, decreasing to 0.010% and 0.002% for 2% and 5%, respectively. For mass fractions of 10% and above, the uncertainty remained at 0.001%.

Density measurements were carried out with a DMA 4500 density analyzer (Anton Paar GmbH, Graz, Austria), which operates on the oscillating U-tube principle. The instrument, presented in Figure 1a, allows density to be determined in accordance with PN-EN ISO 12185:2024-08+Ap1:2025-08 [32]. The measurement temperature could be controlled with an accuracy of 0.02 °C, while the stated density measurement accuracy was 5×10^{-5} g/cm^3.



(a) (b)

Figure 1. Instruments used for density and kinematic viscosity measurements [37]: (**a**) Anton Paar DMA 4500 density analyzer; (**b**) Labovisco bv TV 2000 viscometer bath.

Kinematic viscosity was evaluated using a Cannon-Fenske Opaque glass capillary viscometer (Paradise Scientific Company Ltd., Dhaka, Bangladesh) thermostated in a TV 2000 viscometer bath (Labovisco bv, Zoetermeer, The Netherlands), shown in Figure 1b. The measurement procedure was conducted in accordance with PN-EN ISO 3104:2024-01 [33]. According to the instrument calibration documentation, the temperature control accuracy was 0.01 °C and the viscosity measurement accuracy was 0.1 mm^2/s.

The environmental conditions during the tests were as follows: air temperature of 21 °C and atmospheric pressure of 1021 hPa.

Kinematic viscosity and density were measured for each sample at temperatures of 40, 50, 60, 70, 80, 90, and 100 °C, after which the dynamic viscosity was calculated. The measurement instruments used in the study are shown in Figure 1.

The dynamic viscosity was determined from the measured kinematic viscosity and density of each sample. These parameters are related by the following equation [32,33]:

$$\eta = \nu \cdot \rho, \tag{1}$$

where η is the dynamic viscosity, ν is the kinematic viscosity, and ρ is the density of the sample.

Accordingly, the dynamic viscosity for each sample and measurement temperature was calculated as the product of the experimentally determined kinematic viscosity and density. Detailed results of the kinematic viscosity, dynamic viscosity and density measurements and measurement uncertainties are provided in Appendix A.

2.2. Investigated Models

Power-law models describe the dynamic viscosity η_{blend} of an n-component liquid mixture, in which the i-th component has a dynamic viscosity η_i and contributes a mass fraction x_i to the mixture, according to the following relationship:

$$(\eta_{blend})^k = \sum_{i=1}^{n} x_i \eta_i^k, \tag{2}$$

where k is the exponent of the power-law model, and η_{blend} is the dynamic viscosity of the mixture.

For a binary mixture, n = 2, Equation (2) can be written in the following form:

$$\eta_{blend} = \sqrt[k]{x_1 \eta_1^k + x_2 \eta_2^k}, \tag{3}$$

where η_1 and η_2 are the dynamic viscosities of components 1 and 2, respectively, and x_1 and x_2 are their corresponding mass fractions. In the present study, component 1 denotes the lubricating oil (LO), whereas component 2 represents the diesel oil (DO).

Taking into account that $x_1 + x_2 = 1$, Equation (3) takes the following form:

$$\eta_{blend} = \sqrt[k]{x_1\eta_1^k + (1 - x_1)\eta_2^k}, \quad (4)$$

The simplest case, obtained for $k = 1$, corresponds to the linear blending relationship:

$$\eta_{blend} = x_1\eta_1 + (1 - x_1)\eta_2, \quad (5)$$

Another model reported in the literature is the Kendall and Monroe equation, for which $k = 1/3$, resulting in the following relationship:

$$\eta_{blend} = \left(x_1\eta_1^{0.33(3)} + (1 - x_1)\eta_2^{0.33(3)}\right)^3, \quad (6)$$

The Koval and Bingham equations represent power-law models with negative values of the exponent. For the Koval model, $k = -1/4$, and the corresponding relationship is:

$$\eta_{blend} = \frac{1}{\left(\frac{x_1}{\eta_1^{0.25}} + \frac{1-x_1}{\eta_2^{0.25}}\right)^4}, \quad (7)$$

For the Bingham equation, $k = -1$, and Equation (3) takes the following form:

$$\eta_{blend} = \frac{1}{\frac{x_1}{\eta_1} + \frac{1-x_1}{\eta_2}}, \quad (8)$$

For comparison purposes, two additional viscosity models, namely the Arrhenius and REFUTAS models, were also considered. The Arrhenius model describes the viscosity of a binary mixture based on the logarithmic combination of the viscosities of its individual components and their respective mass fractions. For the mixtures investigated in this study, the model is expressed as:

$$\eta_{blend} = \exp[x_1 \ln(\eta_1) + (1 - x_1) \ln(\eta_2)], \quad (9)$$

The REFUTAS model was also included as a reference method. Unlike the models described above, REFUTAS is based on kinematic viscosity and uses the Viscosity Blending Index (*VBI*) to estimate the viscosity of a mixture. The *VBI* of each component is calculated from its kinematic viscosity according to:

$$VBI_1 = 14.534 \cdot \ln[\ln(\eta_1 + 0.8)] + 10.975, \quad (10)$$

$$VBI_2 = 14.534 \cdot \ln[\ln(\eta_2 + 0.8)] + 10.975, \quad (11)$$

For the binary mixture considered in this study, the VBI_{blend} of the blend is determined from the mass-weighted contributions of the two components:

$$VBI_{blend} = x_1 VBI_1 + (1 - x_1)VBI_2, \quad (12)$$

The kinematic viscosity of the mixture is then obtained by rearranging the VBN relationship:

$$\nu_{blend} = \exp\left[\exp\left(\frac{VBI_{blend} - 10.975}{14.534}\right)\right] - 0.8, \quad (13)$$

where ν_{blend} denotes the predicted kinematic viscosity of the mixture [40], and the corresponding dynamic viscosity can subsequently be calculated from the mixture density using Equation (1).

The Arrhenius and REFUTAS models were treated as reference models, and their predictions were compared with the experimentally determined dynamic viscosity values to assess their ability to reproduce the viscosity behavior of the investigated binary mixtures.

2.3. Evaluation of Model Prediction Accuracy

The accuracy of the viscosity models was assessed by comparing the dynamic viscosity values predicted by each model with the corresponding experimental measurements. Three complementary statistical measures were used: the root mean square relative error (*RMSRE*), the maximum relative error (*MRE*), and the coefficient of determination (R^2).

RMSRE and provides an overall assessment of the deviations between the model predictions and experimental results, whereas the maximum relative percentage error *MRE* indicates the largest relative deviation observed within the analyzed dataset. The coefficient of determination (R^2) was used as an additional measure of the degree of agreement between the calculated and experimentally measured viscosity values. The *RMSRE* was calculated according to:

$$RMSRE = \sqrt{\frac{1}{m}\sum_{i=1}^{m}\left(\eta_{i,model} - \eta_{i,exp}\right)^2}\cdot 100\%, \quad (14)$$

where m is the number of experimental observations, $\eta_{i,model}$ is the dynamic viscosity predicted by the model for the i-th observation, and $\eta_{i,exp}$ is the corresponding experimentally measured dynamic viscosity.

The maximum percentage relative error *MRE* was determined according to:

$$MRE = \max_i\left(\frac{\eta_{i,model} - \eta_{i,exp}}{\eta_{i,exp}}\cdot 100\%\right), \quad (15)$$

The coefficient of determination R^2 was calculated to quantify the proportion of the variability in the experimental viscosity values that is represented by the model predictions. The R^2 values were subsequently used as a complementary measure in the comparative assessment of the investigated models.

Lower values of *RMSRE* and *MRE* indicate better agreement between the model predictions and the experimental data, whereas higher values of R^2 indicate a stronger correspondence between the calculated and experimental values. The simultaneous application of these three measures allows the models to be evaluated from complementary perspectives, considering the magnitude of prediction errors, the largest relative deviation, and the overall correspondence between calculated and experimental values.

3. Results and Discussion

The applicability of the investigated models was assessed by comparing the experimentally determined dynamic viscosity of the lubricating oil–diesel oil mixtures with values calculated using each of the six considered models. The analysis was performed separately for SAE 30 and SAE 40 lubricating oils over the entire investigated range of diesel oil contamination (0–100% m/m) and temperature (40–100 °C).

The selected physical and rheological properties of the investigated mixtures are provided in Appendix A, while the dynamic viscosity values calculated using the investigated models are presented in Appendix B.

For each model, two complementary approaches were used to evaluate its predictive performance. First, scatter plots of the calculated dynamic viscosity against the experimentally measured viscosity were prepared. In these plots, the line (y = x) represents perfect agreement between calculated and experimental values; therefore, the closer the data points are to this line, the better the predictive performance of the model. Second, three-dimensional surfaces of the relative error were generated as a function of diesel oil contamination and temperature. These surfaces provide additional information on the distribution of the model error over the investigated experimental domain and allow the ranges of temperature and contamination associated with higher or lower prediction accuracy to be identified.

The results obtained for the six investigated models are presented and discussed separately below. The linear, Kendall–Monroe, Koval and Bingham models represent the power-law approach, whereas the Arrhenius and REFUTAS models are considered as reference models. The latter two models are particularly relevant because their inverse formulations have previously been investigated for estimating diesel oil concentration in lubricating oil.

3.1. Linear Model

The comparison between the experimentally measured dynamic viscosity and the values calculated using the linear model is presented in Figures 2 and 3 for SAE 30 and SAE 40 lubricating oils, respectively. The corresponding distributions of the relative error over the investigated ranges of diesel oil contamination and temperature are shown in Figures 4 and 5.

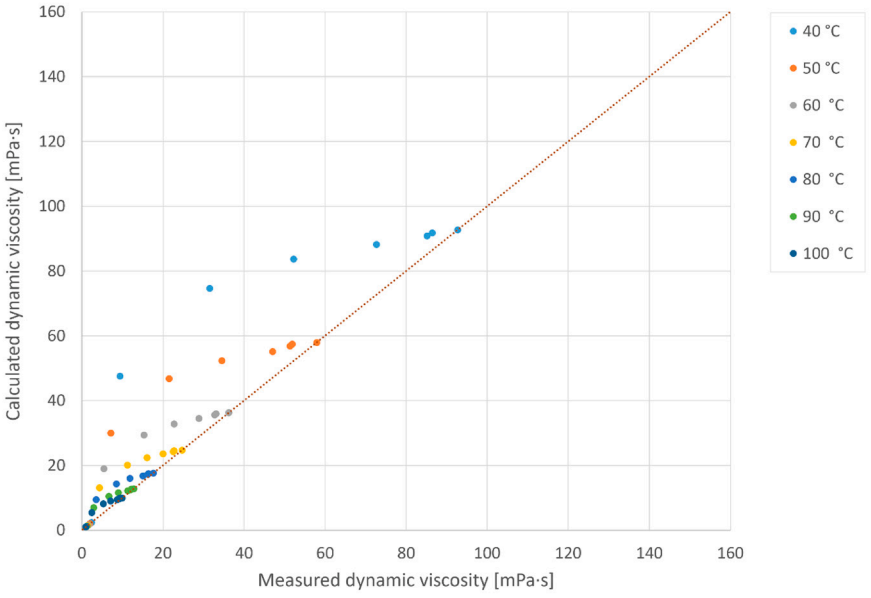


Figure 2. Comparison of experimentally measured and calculated dynamic viscosity for SAE 30 lubricating oil using the linear model. The dashed line represents perfect agreement (y = x)

The scatter plots show the degree of agreement between the calculated and experimental viscosities for both lubricating oils. The distribution of points relative to the (y = x) line indicates the extent to which the linear relationship is capable of reproducing the experimentally observed viscosity of the binary mixtures. The calculated values are predominantly located above the (y = x) line, indicating a clear tendency of the linear model to overestimate the experimentally measured viscosity. Deviations from the reference line become particularly important when considering the complete range of diesel oil contami-

nation and temperature, demonstrating that the simple linear relationship does not fully reproduce the non-linear viscosity behaviour of the investigated mixtures.

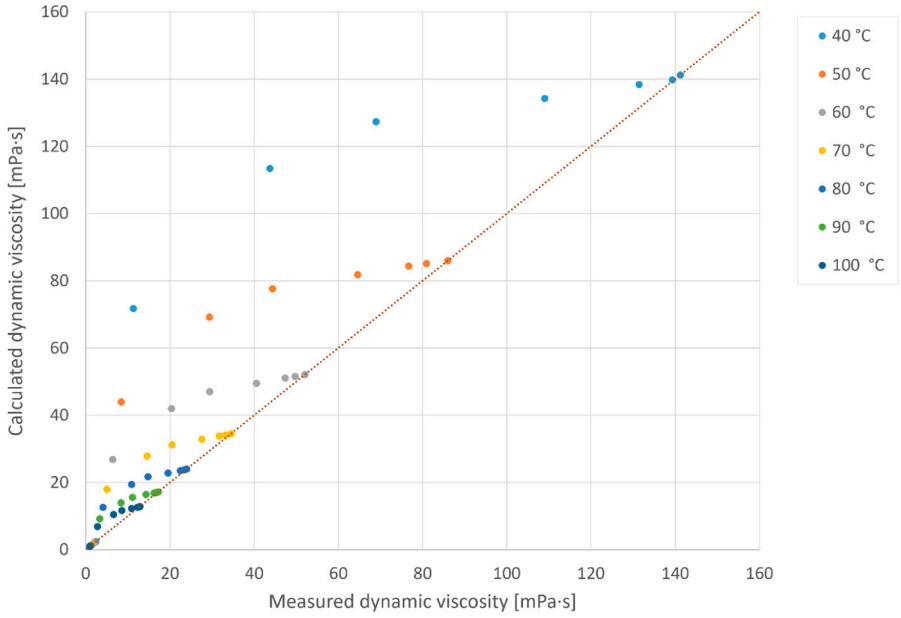


Figure 3. Comparison of experimentally measured and calculated dynamic viscosity for SAE 40 lubricating oil using the linear model. The dashed line represents perfect agreement (y = x).

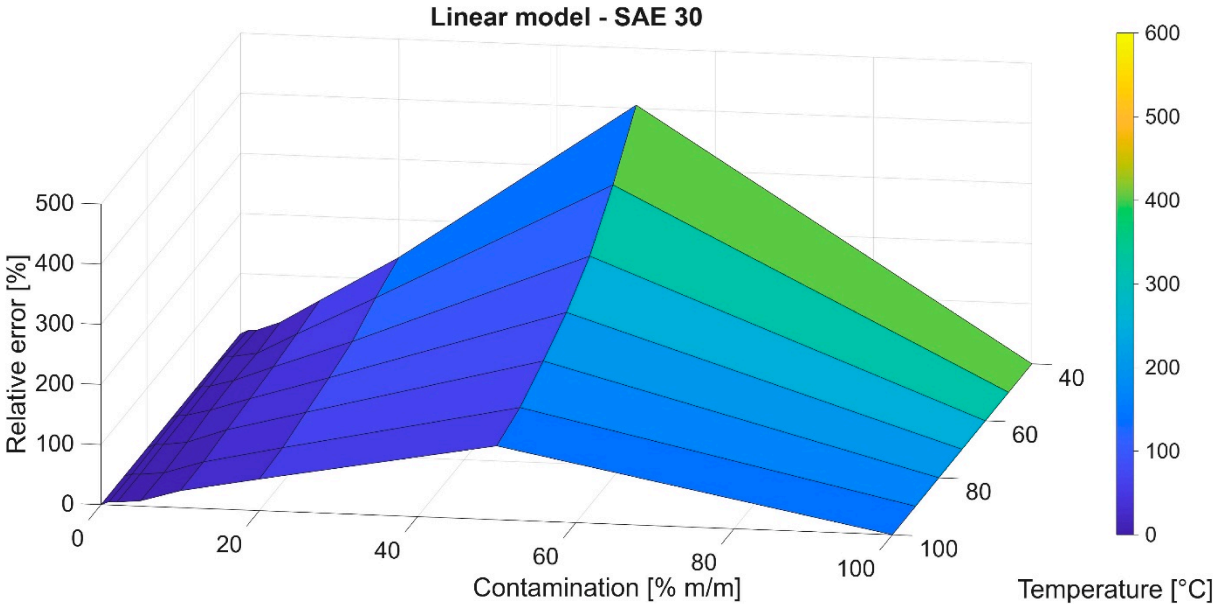


Figure 4. Relative error of dynamic viscosity calculated using the linear model for SAE 30 lubricating oil as a function of diesel oil contamination and temperature.

This observation is confirmed by the relative-error surfaces shown in Figures 4 and 5. The error is not constant throughout the investigated experimental domain but varies with both diesel oil contamination and temperature. The maximum relative error reached 405.19% for SAE 30 and 537.35% for SAE 40. The independently calculated *RMSRE* values were 95.02% and 122.31%, respectively. This indicates that the accuracy of the linear model cannot be characterised by a single representative value without losing information about its dependence on mixture composition and temperature. Among the six investigated models, the linear model provided the lowest overall accuracy and therefore represents

the least suitable formulation for describing the viscosity of the investigated lubricating oil–diesel oil mixtures.

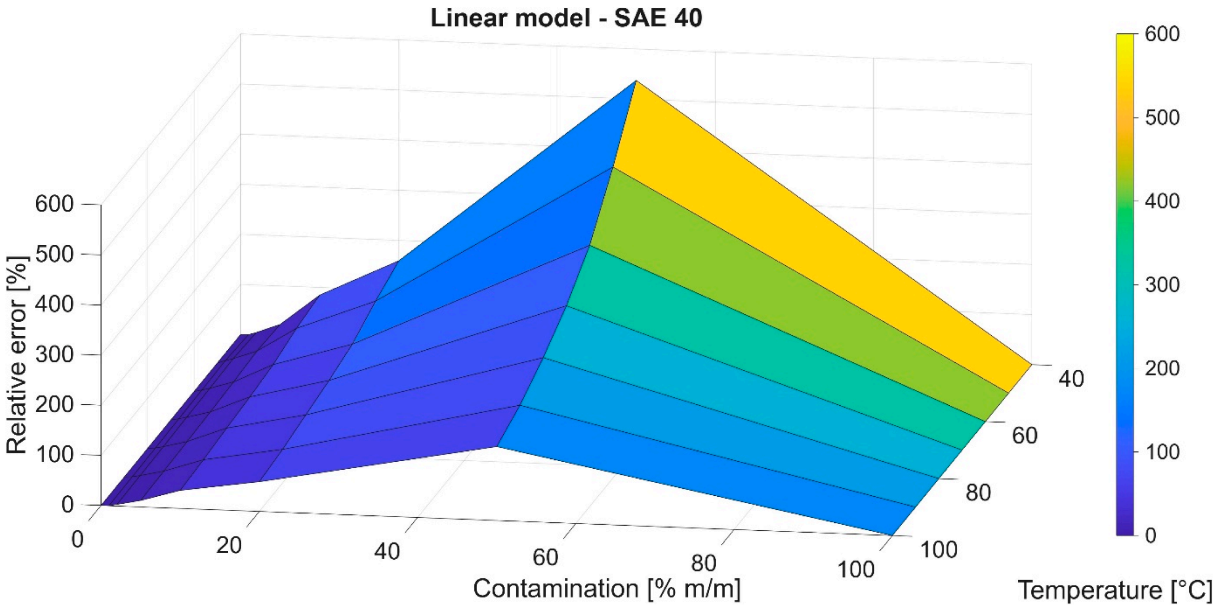


Figure 5. Relative error of dynamic viscosity calculated using the linear model for SAE 40 lubricating oil as a function of diesel oil contamination and temperature.

3.2. Kendall and Monroe Model

The performance of the Kendall–Monroe model is illustrated in Figures 6–9. Figures 6 and 7 present the calculated versus experimentally measured dynamic viscosity for SAE 30 and SAE 40, respectively, whereas Figures 8 and 9 show the corresponding relative-error surfaces.

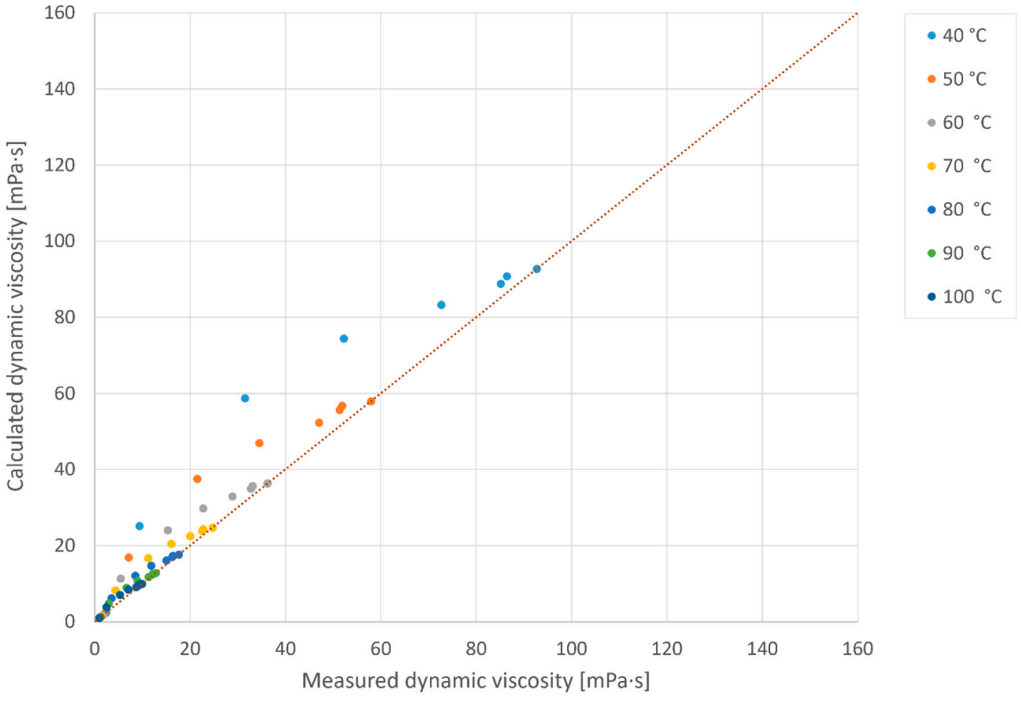


Figure 6. Comparison of experimentally measured and calculated dynamic viscosity for SAE 30 lubricating oil using the Kendall–Monroe model. The dashed line represents perfect agreement (y = x).

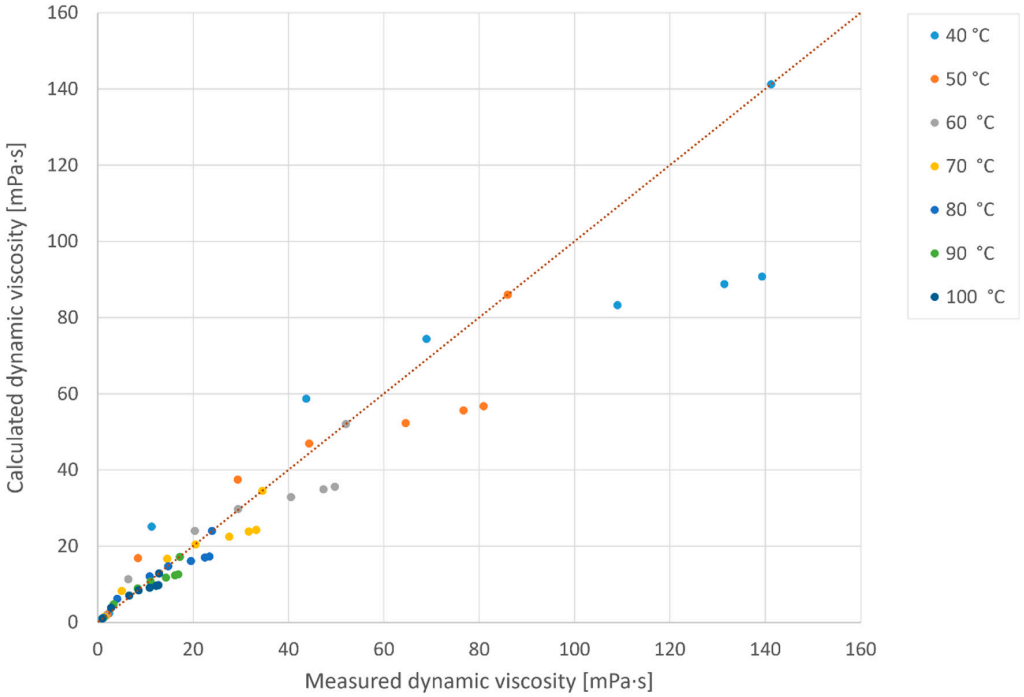


Figure 7. Comparison of experimentally measured and calculated dynamic viscosity for SAE 40 lubricating oil using the Kendall–Monroe model. The dashed line represents perfect agreement (y = x).

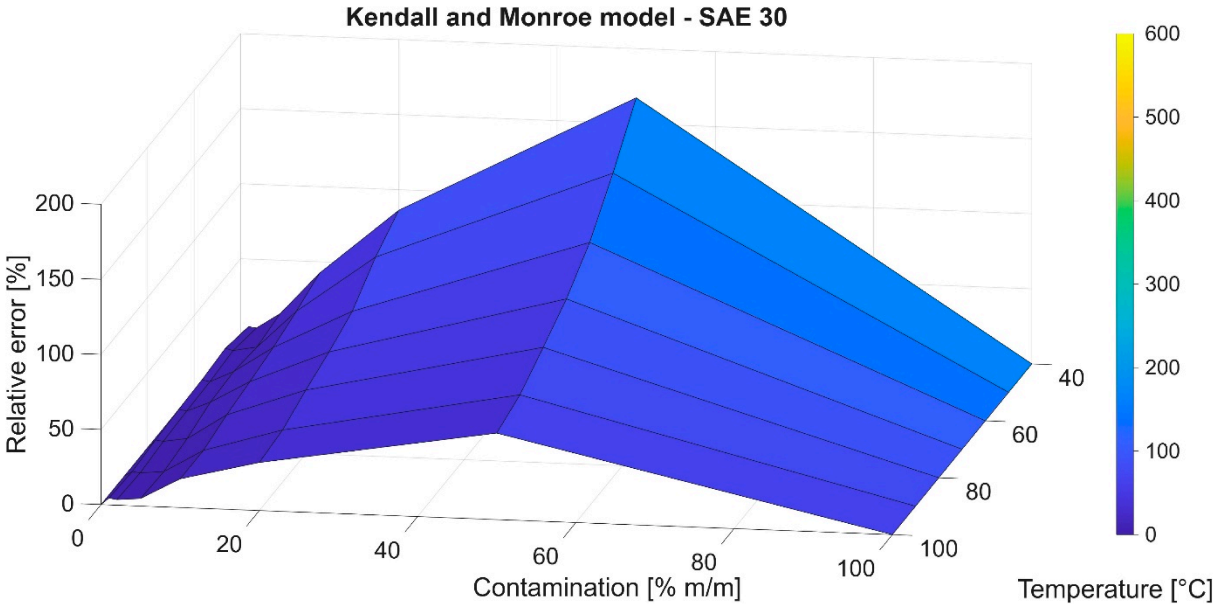


Figure 8. Relative error of dynamic viscosity calculated using the Kendall–Monroe model for SAE 30 lubricating oil as a function of diesel oil contamination and temperature.

Compared with the linear model, the Kendall–Monroe relationship provides a different representation of the contribution of the individual components to mixture viscosity. The scatter plots in Figures 5 and 6 show an improved agreement between calculated and experimental values compared with the linear formulation, although noticeable deviations from the (y = x) line remain over part of the investigated range. The calculated values occur both above and below the (y = x) line, indicating that the model both overestimates and underestimates the experimentally measured viscosity, depending on the investigated conditions.

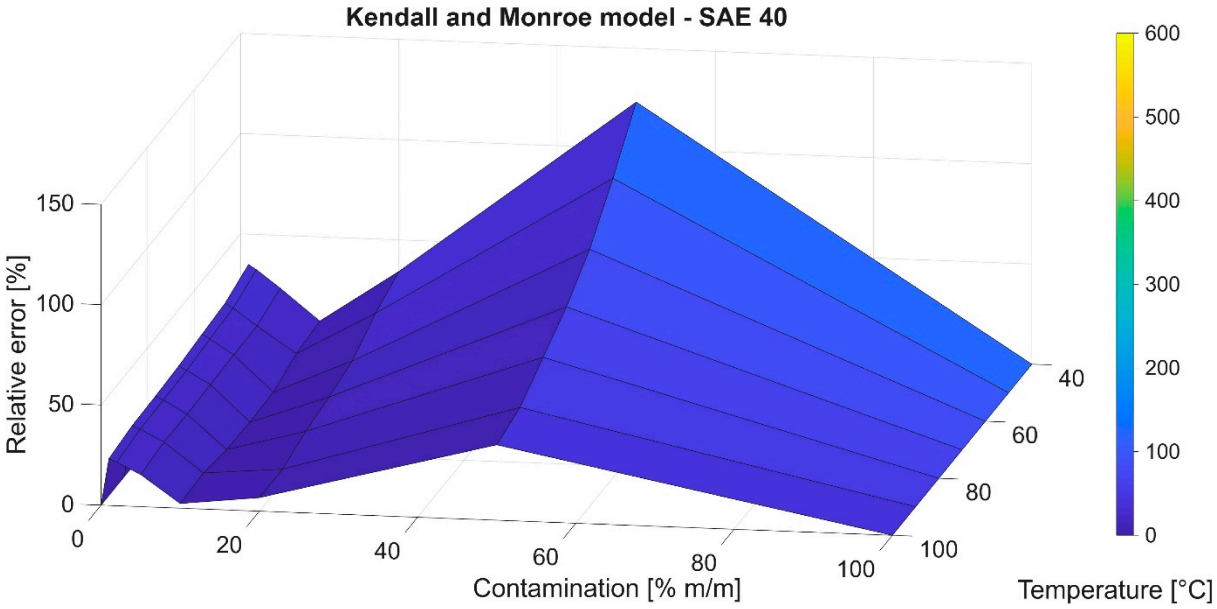


Figure 9. Relative error of dynamic viscosity calculated using the Kendall–Monroe model for SAE 40 lubricating oil as a function of diesel oil contamination and temperature.

The relative-error surfaces in Figures 7 and 8 confirm that the model accuracy depends on both temperature and diesel oil contamination. As shown in Figures 8 and 9, the maximum relative error reached 167.23% for SAE 30 and 123.22% for SAE 40. The independently calculated *RMSRE* values were 44.26% and 31.86%, respectively. The model therefore provides a more adequate representation of the viscosity behaviour than the linear relationship, but its predictive capability remains limited compared with the more accurate formulations considered in this study. On the basis of the complete experimental domain, the Kendall–Monroe model ranked second among the least accurate power-law formulations.

3.3. Koval Model

The results obtained using the Koval model are presented in Figures 10–13. The calculated and measured dynamic viscosities for SAE 30 and SAE 40 are compared in Figures 10 and 11, while Figures 12 and 13 present the corresponding relative-error surfaces.

The Koval model shows a substantially better agreement with the experimental data than the previously discussed power-law formulations. As illustrated in Figures 9 and 10, the calculated values are concentrated more closely around the (y = x) line for both lubricating oil grades. The points are distributed closely around the reference line without a pronounced systematic displacement in either direction, indicating a close agreement between the calculated and experimental viscosities. This indicates that the model more effectively reproduces the experimentally observed dependence of dynamic viscosity on mixture composition and temperature.

The improved performance of the Koval model is also evident from the relative-error surfaces shown in Figures 12 and 13. The calculated relative errors remain comparatively low over the investigated temperature and contamination ranges, although their magnitude is not completely independent of mixture composition and temperature. As shown in Figures 12 and 13, the maximum relative error was 6.84% for SAE 30 and 8.42% for SAE 40. The independently calculated *RMSRE* values were 3.28% and 3.07%, respectively. The maximum relative error obtained for the Koval model was below 9%, making it the most accurate of the investigated power-law models.

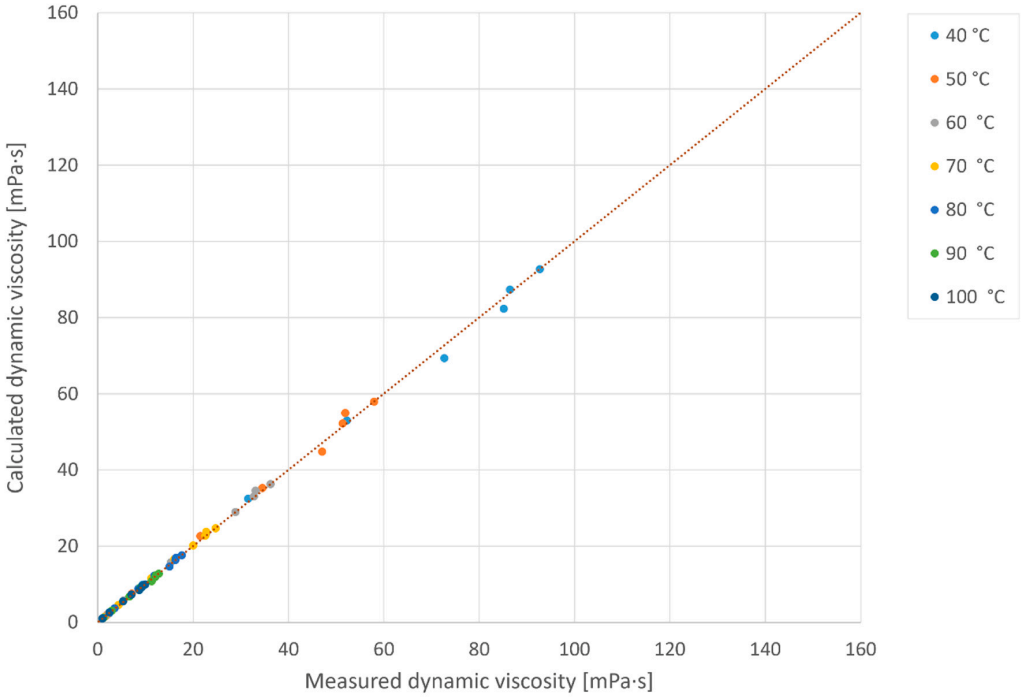


Figure 10. Comparison of experimentally measured and calculated dynamic viscosity for SAE 30 lubricating oil using the Koval model. The dashed line represents perfect agreement (y = x).

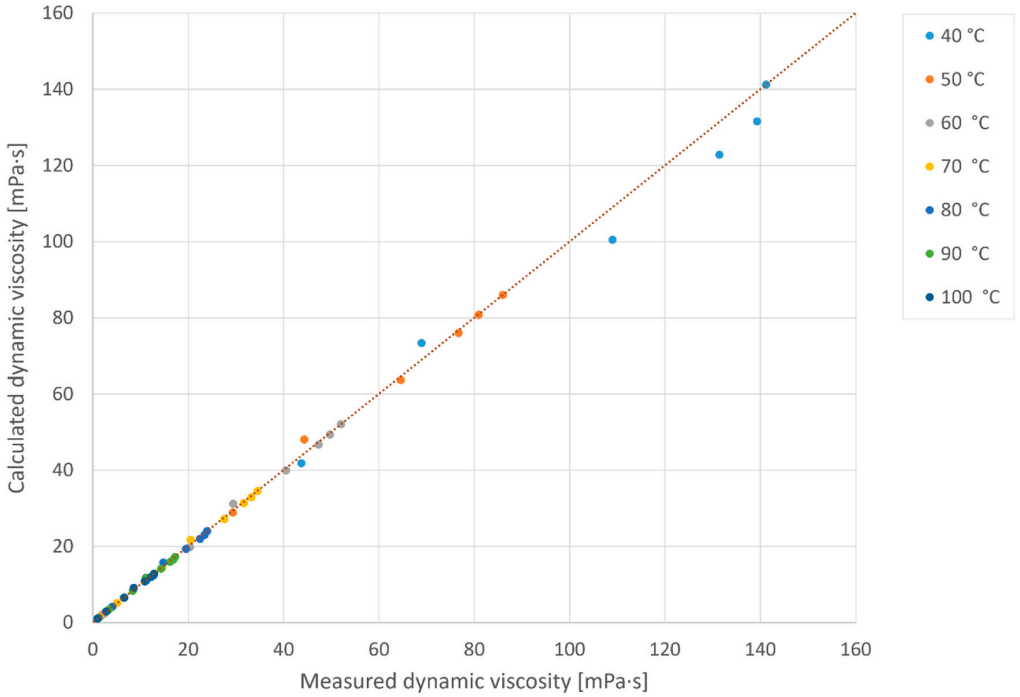


Figure 11. Comparison of experimentally measured and calculated dynamic viscosity for SAE 40 lubricating oil using the Koval model. The dashed line represents perfect agreement (y = x).

Importantly, the accuracy achieved by the Koval model was also higher than that obtained with the Arrhenius model considered as a reference. Its performance was close to that of the REFUTAS model, which was previously shown to provide high accuracy in the inverse estimation of diesel oil concentration in lubricating oil. This result is particularly relevant from a practical perspective because the Koval model retains the relatively simple mathematical form characteristic of power-law models while providing predictive accuracy comparable to that of a substantially more advanced formulation.

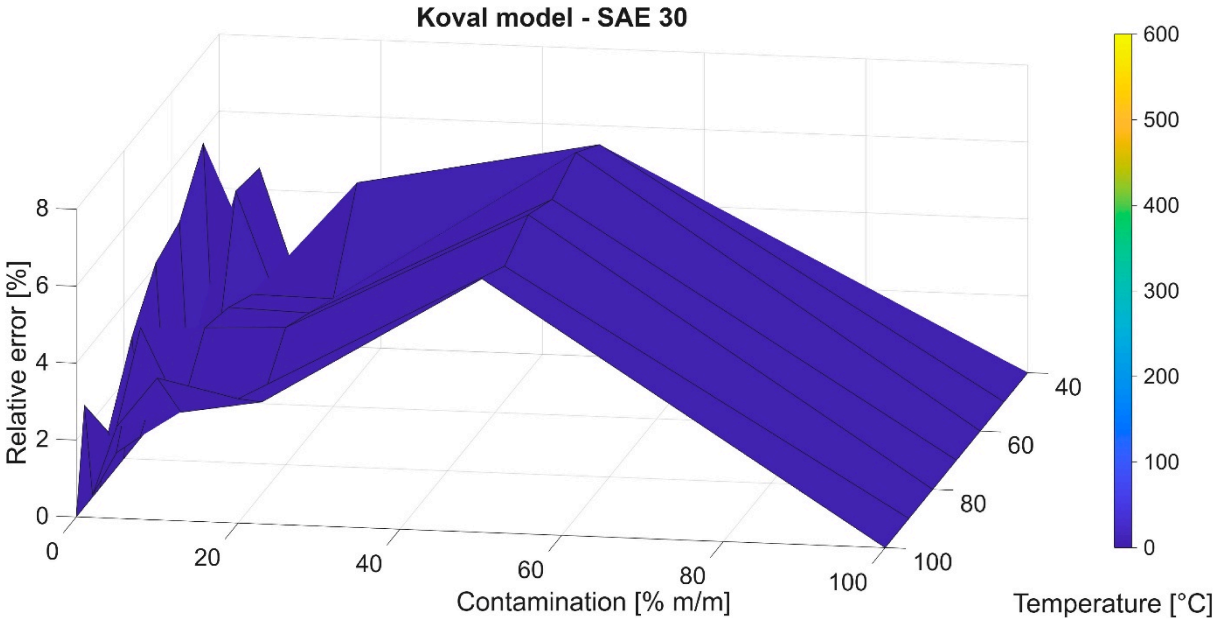


Figure 12. Relative error of dynamic viscosity calculated using the Koval model for SAE 30 lubricating oil as a function of diesel oil contamination and temperature.

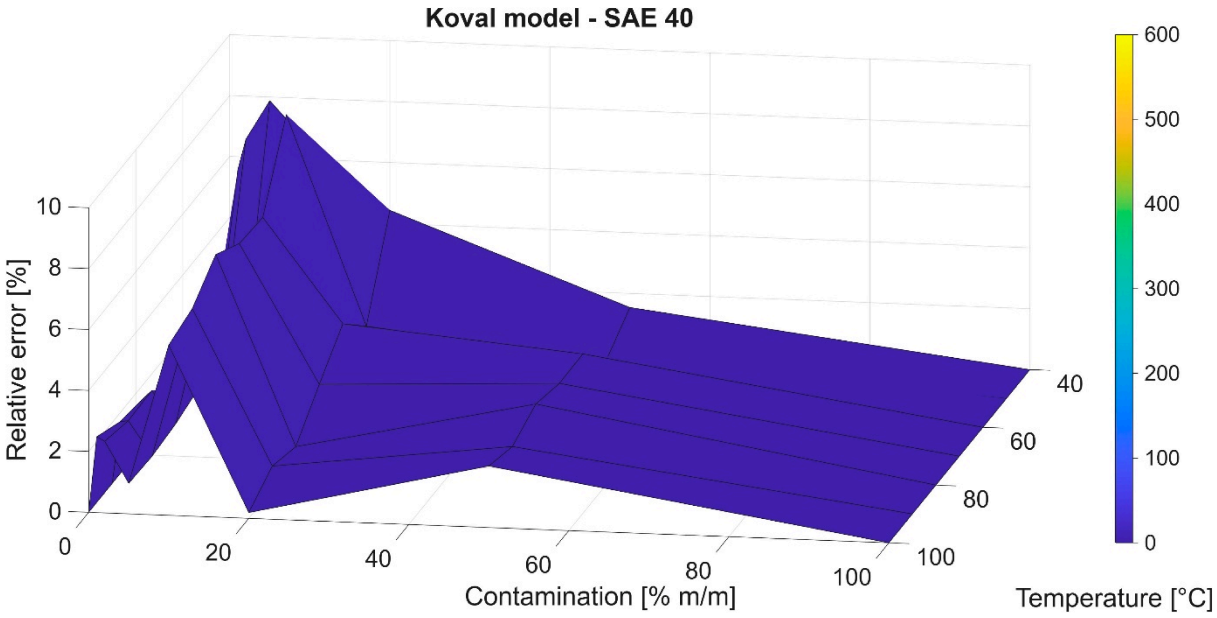


Figure 13. Relative error of dynamic viscosity calculated using the Koval model for SAE 40 lubricating oil as a function of diesel oil contamination and temperature.

3.4. Bingham Model

The results for the Bingham model are shown in Figures 14–17. Figures 14 and 15 compare calculated and experimentally measured dynamic viscosities for SAE 30 and SAE 40, respectively, while Figures 16 and 17 present the corresponding relative-error surfaces.

The Bingham model provides an intermediate level of agreement between the calculated and experimental viscosities. As shown in Figures 14 and 15, the calculated values follow the experimental data reasonably well over the investigated range, but the scatter around the (y = x) line is greater than that observed for the Koval model. The calculated values are predominantly located below the (y = x) line, indicating a clear tendency of the Bingham model to underestimate the experimentally measured viscosity.

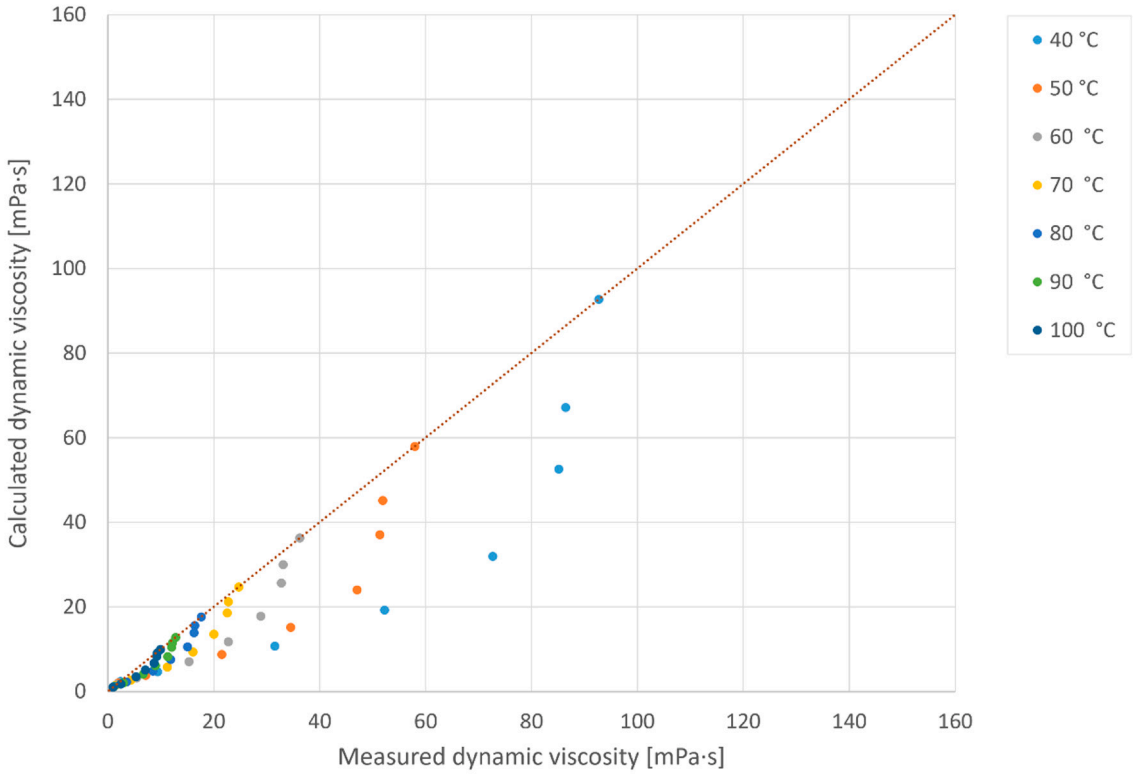


Figure 14. Comparison of experimentally measured and calculated dynamic viscosity for SAE 30 lubricating oil using the Bingham model. The dashed line represents perfect agreement (y = x).

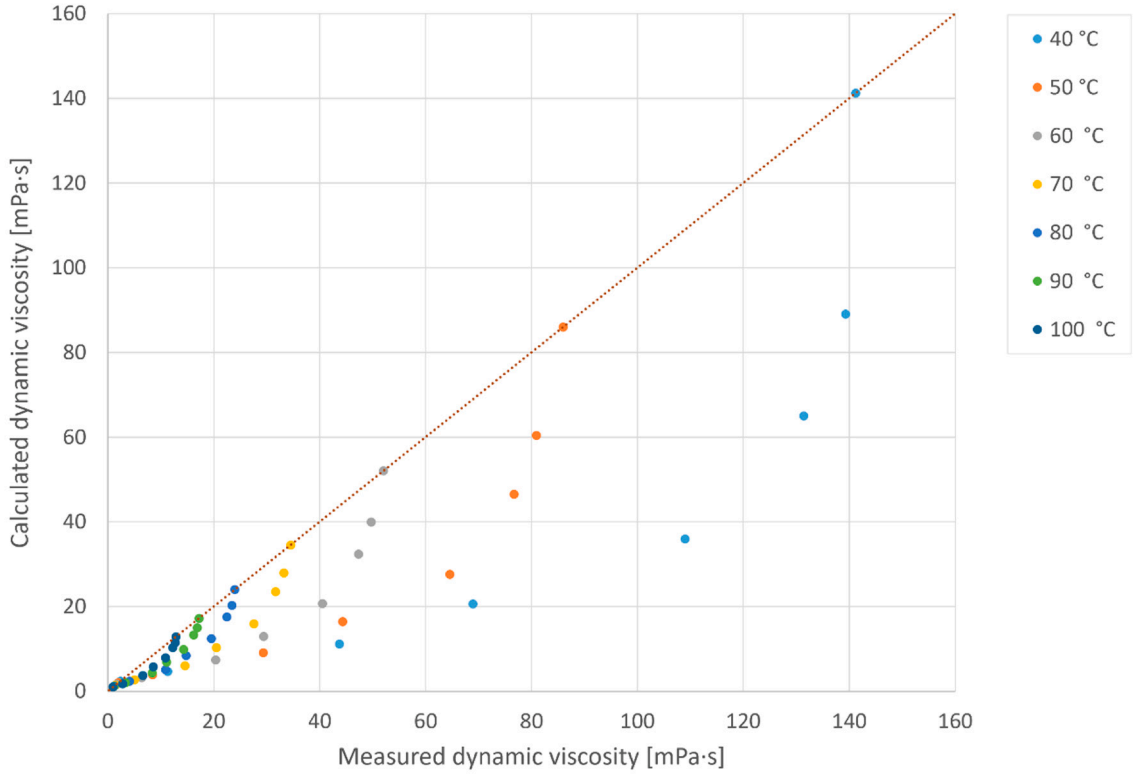


Figure 15. Comparison of experimentally measured and calculated dynamic viscosity for SAE 40 lubricating oil using the Bingham model. The dashed line represents perfect agreement (y = x).

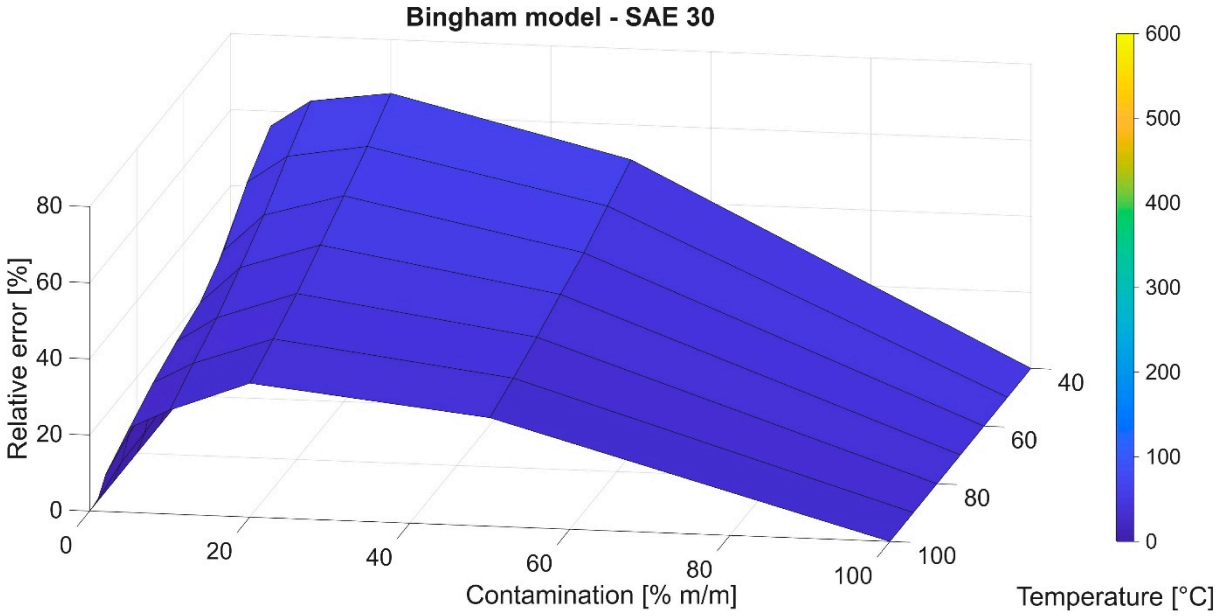


Figure 16. Relative error of dynamic viscosity calculated using the Bingham model for SAE 30 lubricating oil as a function of diesel oil contamination and temperature.

The relative-error surfaces shown in Figures 16 and 17 demonstrate that the discrepancies between calculated and experimental values vary with both temperature and diesel oil contamination. As shown in Figures 16 and 17, the maximum relative error reached 65.88% for SAE 30 and 74.61% for SAE 40. The independently calculated *RMSRE* values were 32.08% and 38.80%, respectively. Thus, although the Bingham relationship provides a useful representation of the viscosity of the binary mixtures, its overall accuracy is lower than that of the Koval model. The comparison of the four power-law formulations indicates that the Koval model provides the most favourable combination of mathematical simplicity and predictive accuracy.

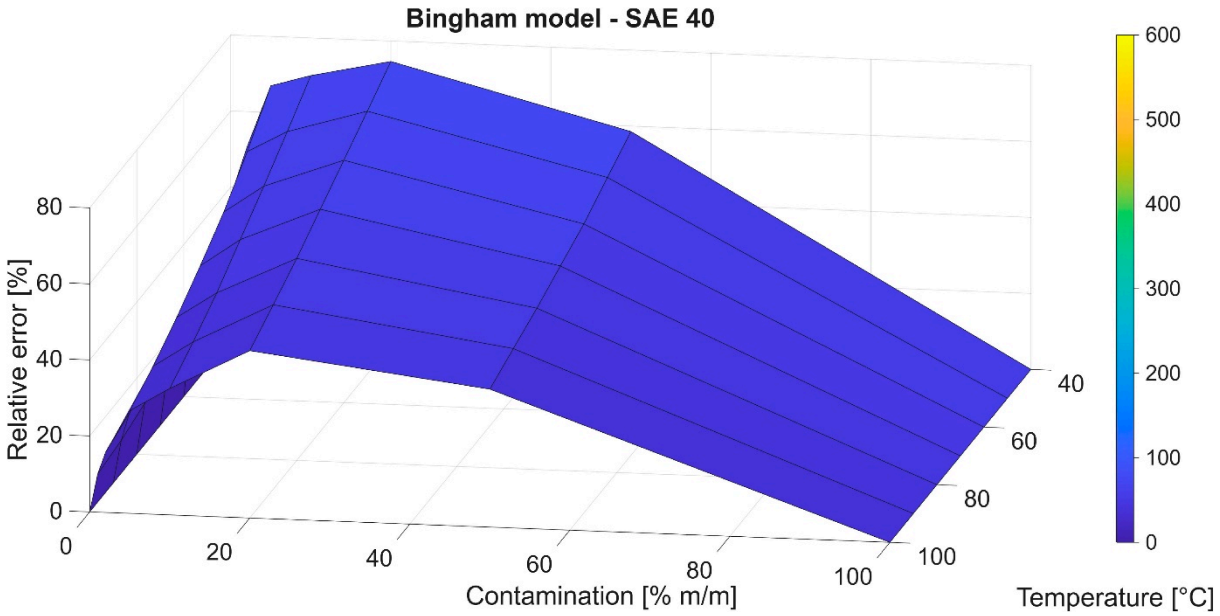


Figure 17. Relative error of dynamic viscosity calculated using the Bingham model for SAE 40 lubricating oil as a function of diesel oil contamination and temperature.

3.5. Arrhenius Model

The Arrhenius model was additionally evaluated as a reference non-power-law formulation. The results for SAE 30 and SAE 40 are presented in Figures 18–21. Figures 18 and 19 show the calculated dynamic viscosity plotted against the experimental values, while Figures 20 and 21 present the relative-error surfaces.

The Arrhenius model provides a good representation of the viscosity of the investigated binary mixtures, as indicated by the relatively close distribution of calculated values around the ($y = x$) line in Figures 18 and 19. The scatter plots show a more frequent occurrence of calculated values above the ($y = x$) line than below it, indicating a tendency toward overestimation of the experimental viscosity. The relative-error surfaces in Figures 20 and 21 further demonstrate that the model provides satisfactory accuracy over the investigated range of temperatures and diesel oil concentrations. As shown in Figures 20 and 21, the maximum relative error reached 57.57% for SAE 30 and 62.45% for SAE 40. The independently calculated *RMSRE* values were 18.61% and 20.60%, respectively.

Despite its good predictive capability, the Arrhenius model was less accurate than the Koval model in the present study. This comparison is important because the Arrhenius relationship was selected as one of the reference models owing to its previous application in the inverse estimation of diesel oil concentration in lubricating oil. The results obtained here therefore indicate that the simpler Koval formulation can reproduce the measured viscosity at least as effectively, and in the investigated range more accurately, than the Arrhenius model.

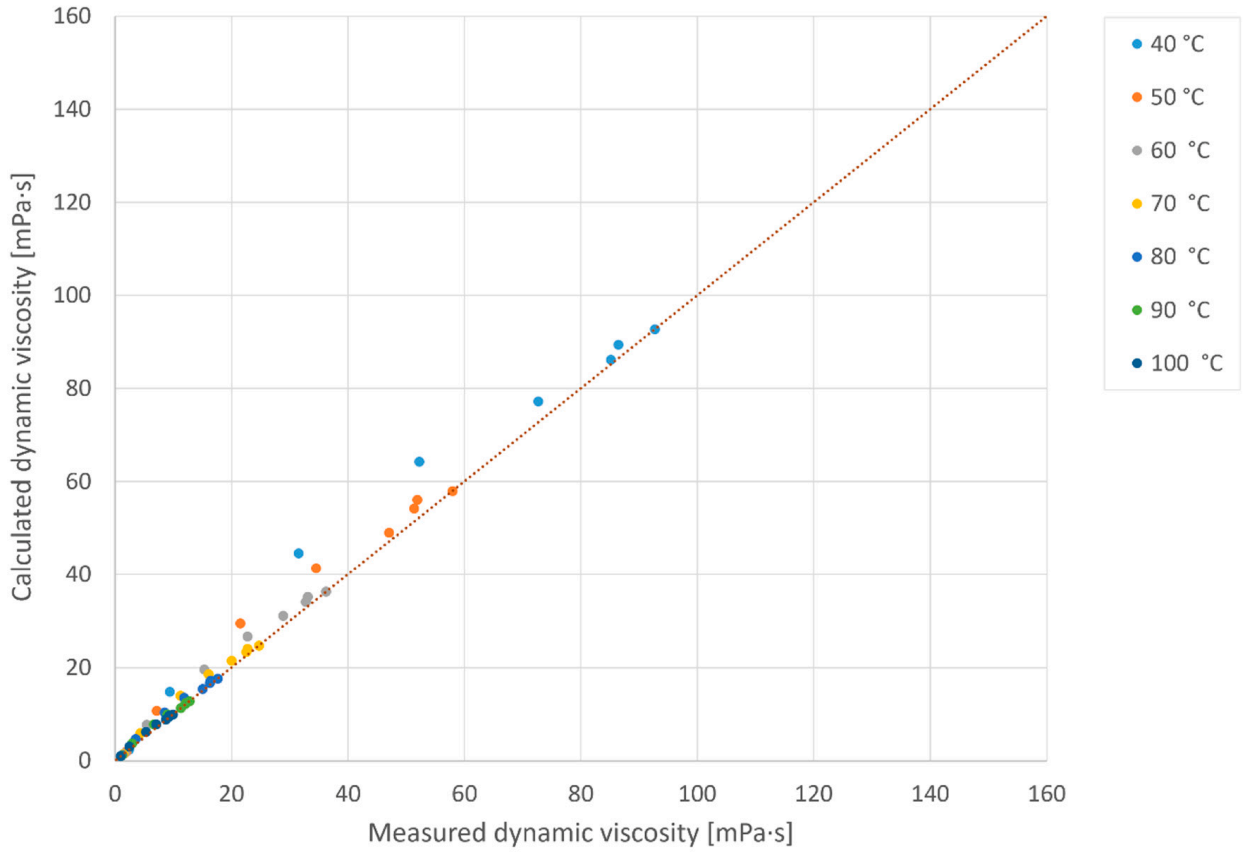


Figure 18. Comparison of experimentally measured and calculated dynamic viscosity for SAE 30 lubricating oil using the Arrhenius model. The dashed line represents perfect agreement (y = x).

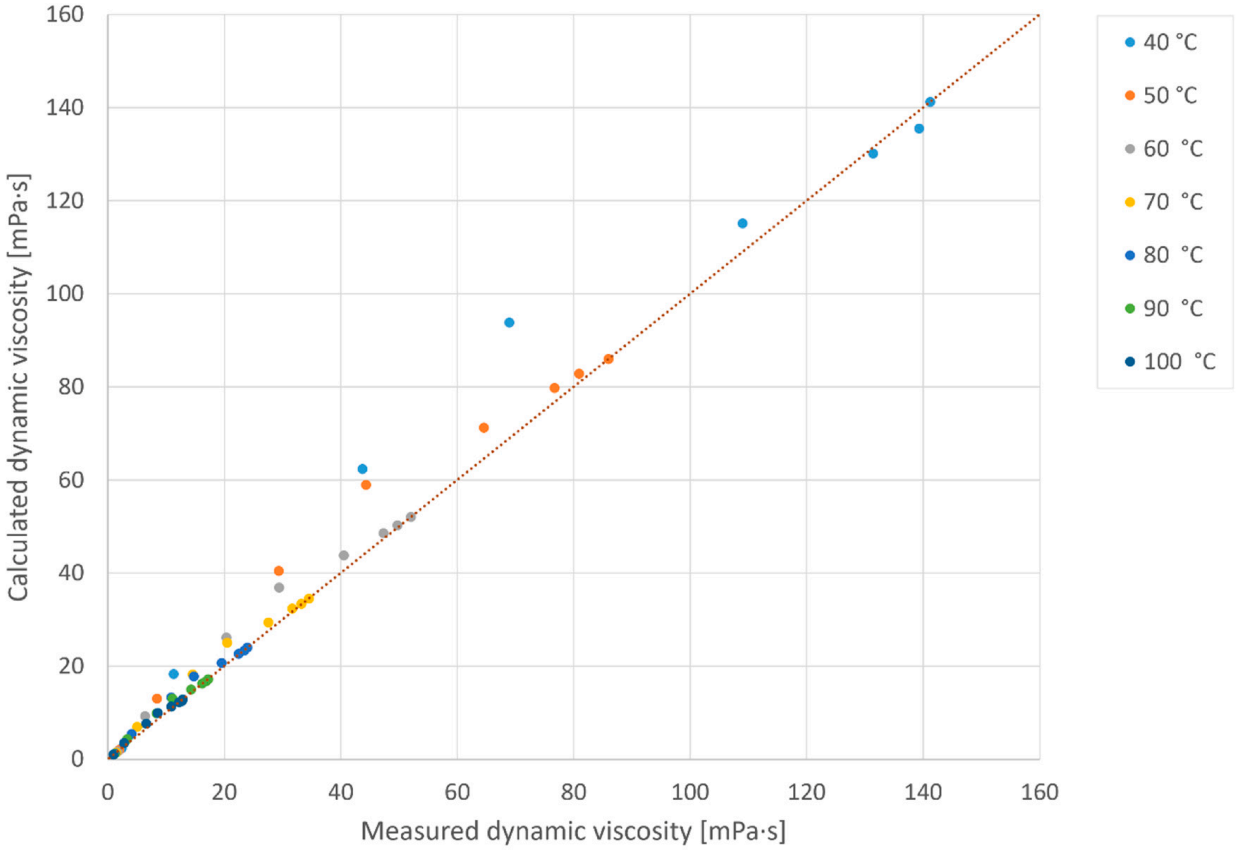


Figure 19. Comparison of experimentally measured and calculated dynamic viscosity for SAE 40 lubricating oil using the Arrhenius model. The dashed line represents perfect agreement (y = x).

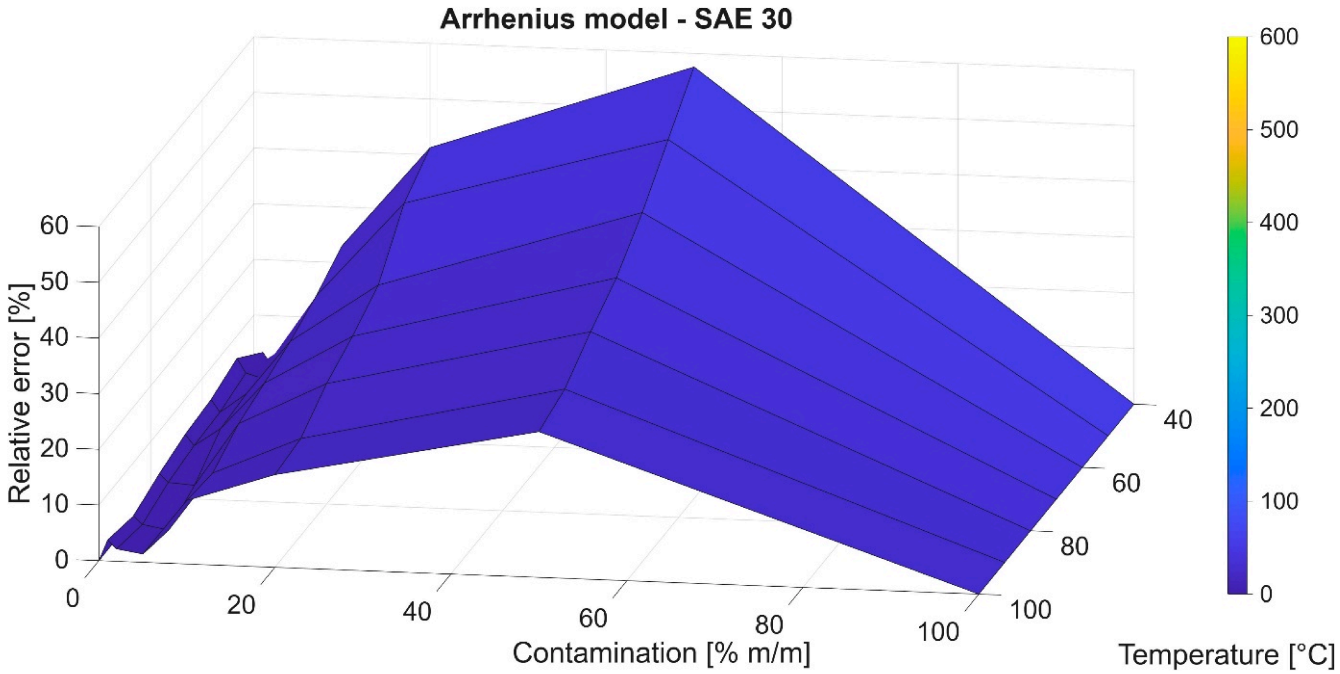


Figure 20. Relative error of dynamic viscosity calculated using the Arrhenius model for SAE 30 lubricating oil as a function of diesel oil contamination and temperature.

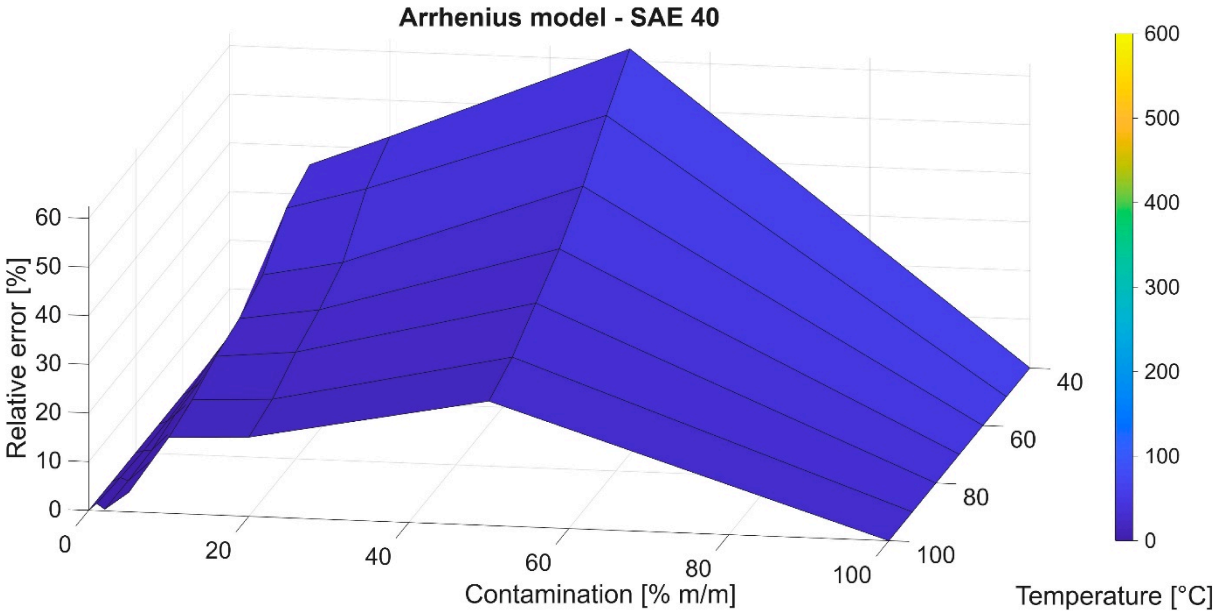


Figure 21. Relative error of dynamic viscosity calculated using the Arrhenius model for SAE 40 lubricating oil as a function of diesel oil contamination and temperature.

3.6. REFUTAS Index Method

The highest-level reference for comparison was provided by the REFUTAS model. The calculated and experimentally measured dynamic viscosities for SAE 30 and SAE 40 are presented in Figures 22 and 23, while the corresponding relative-error surfaces are shown in Figures 24 and 25.

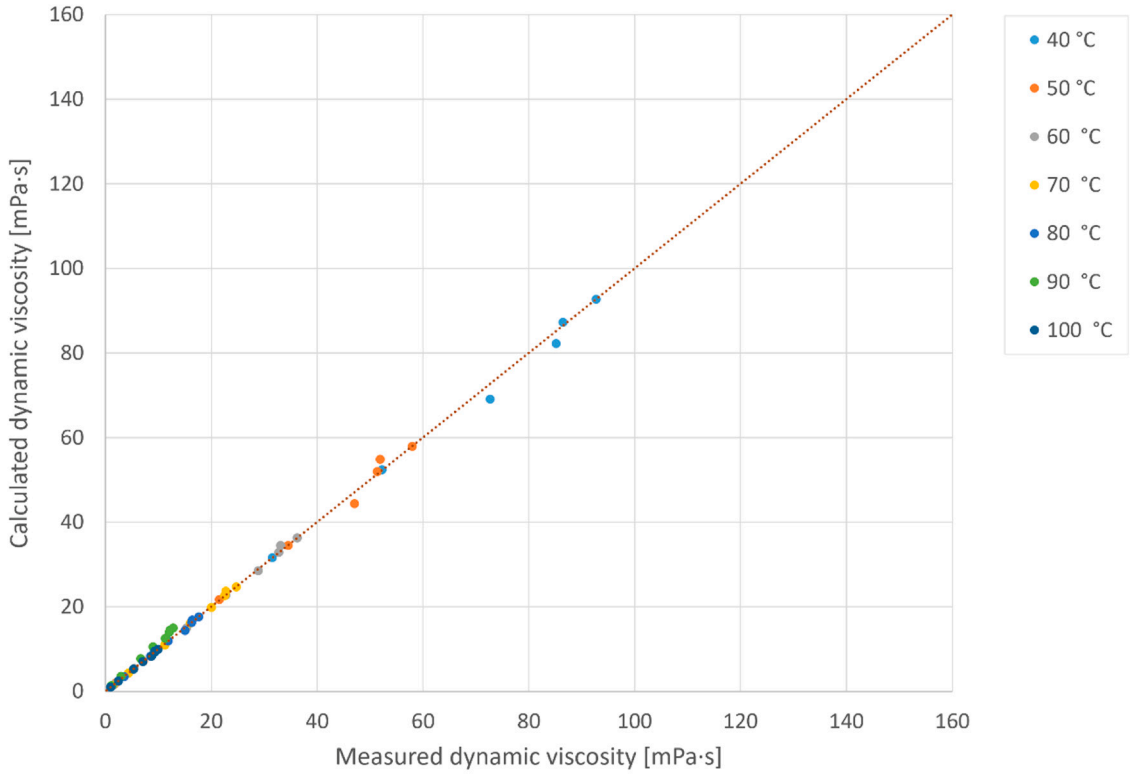


Figure 22. Comparison of experimentally measured and calculated dynamic viscosity for SAE 30 lubricating oil using the REFUTAS model. The dashed line represents perfect agreement (y = x).

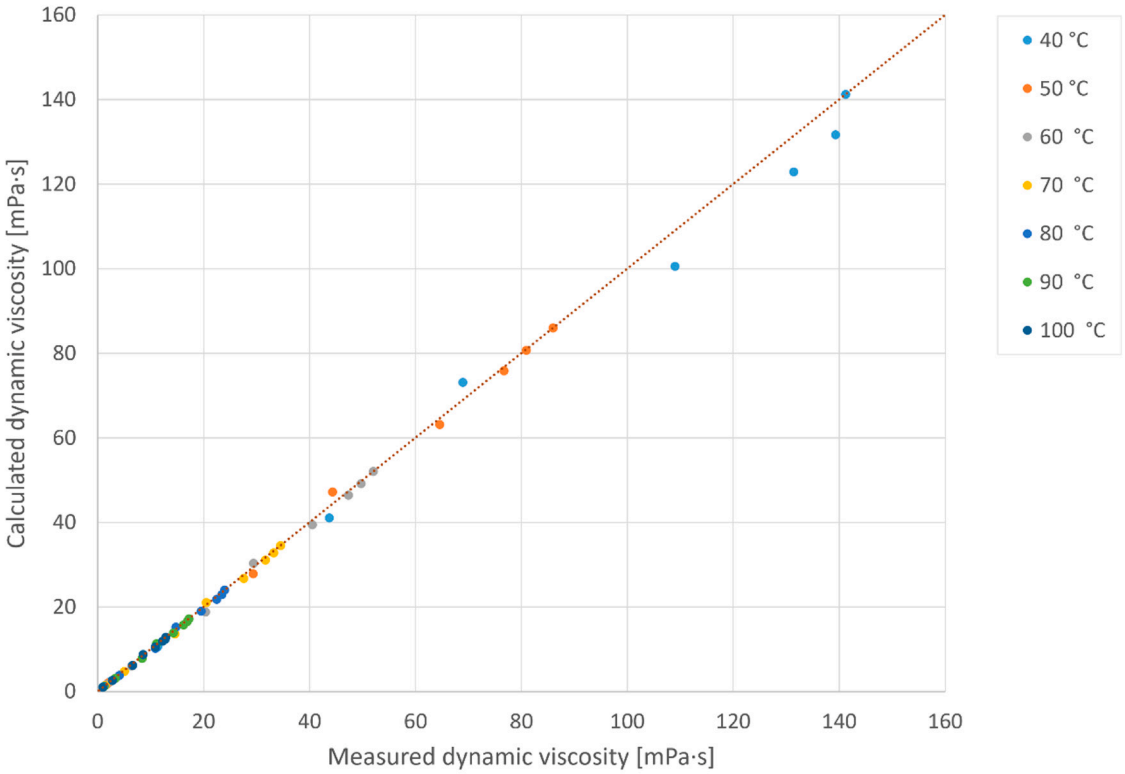


Figure 23. Comparison of experimentally measured and calculated dynamic viscosity for SAE 40 lubricating oil using the REFUTAS model. The dashed line represents perfect agreement (y = x).

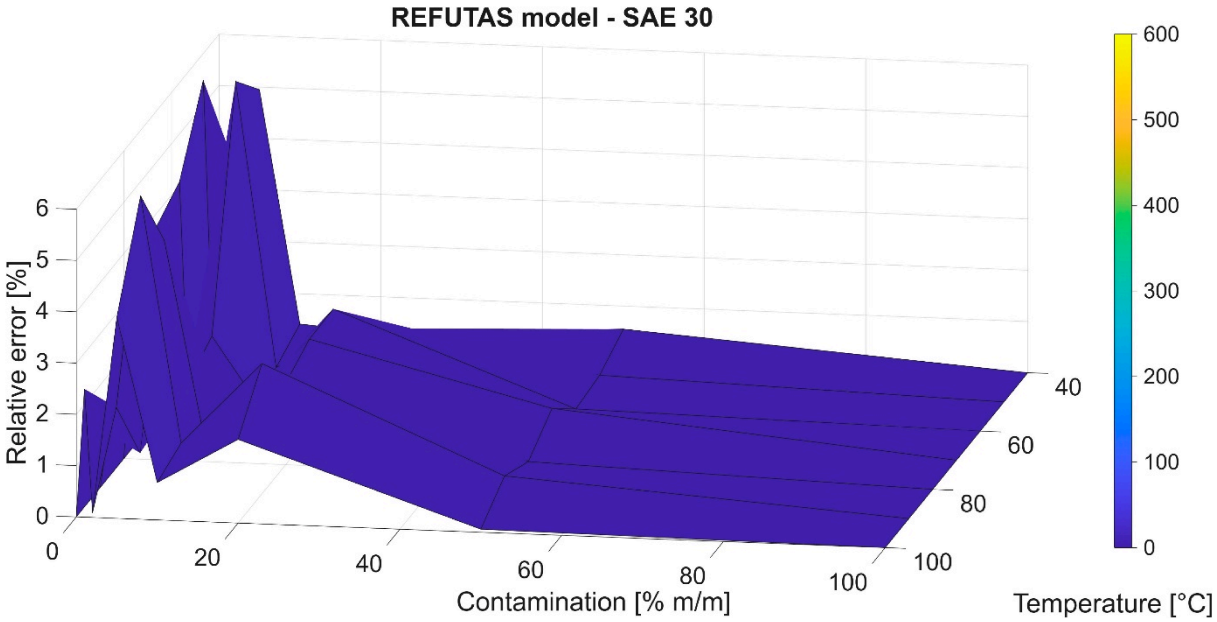


Figure 24. Relative error of dynamic viscosity calculated using the REFUTAS model for SAE 30 lubricating oil as a function of diesel oil contamination and temperature.

The REFUTAS model demonstrates a very good agreement between calculated and experimentally measured dynamic viscosities. The calculated values remain closely distributed around the (y = x) line for both SAE 30 and SAE 40 lubricating oils, indicating a high degree of consistency between the model predictions and the experimental measurements. The scatter plots show a slight predominance of calculated values below the

(y = x) line, indicating a slight tendency of the REFUTAS model to underestimate the experimentally measured viscosity.

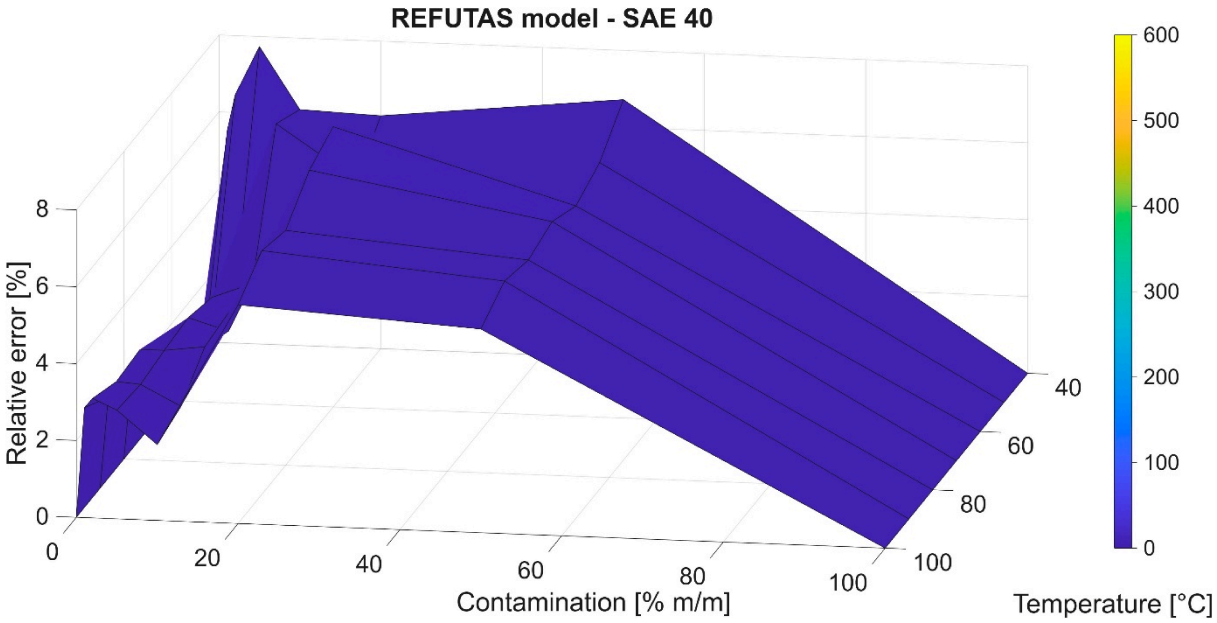


Figure 25. Relative error of dynamic viscosity calculated using the REFUTAS model for SAE 40 lubricating oil as a function of diesel oil contamination and temperature.

This high predictive capability is also reflected in the relative-error surfaces shown in Figures 24 and 25. The maximum relative error was 5.72% for SAE 30 and 7.74% for SAE 40. The independently calculated *RMSRE* values were 2.10% and 3.91%, respectively. The relatively low magnitude of the errors over the investigated temperature and contamination ranges confirms the suitability of the REFUTAS relationship for describing the viscosity behaviour of the tested mixtures. These results are consistent with the previously demonstrated high accuracy of the REFUTAS model in its inverse application for estimating diesel oil concentration in lubricating oil.

3.7. Comparative Assessment of the Investigated Models

The results obtained for all six models demonstrate clear differences in their ability to reproduce the experimentally measured dynamic viscosity of the investigated lubricating oil–diesel oil mixtures. The scatter plots provide a direct visual assessment of the agreement between calculated and measured values, whereas the three-dimensional error surfaces reveal how the prediction accuracy changes with temperature and diesel oil contamination. A quantitative comparison of the models based on the root mean square relative error (*RMSRE*) and maximum relative error (*MRE*) is presented in Figures 26 and 27, respectively.

The quantitative indicators presented in Figures 26 and 27 confirm the differences observed in the graphical analysis. Among the investigated power-law formulations, the linear model showed by far the lowest accuracy, with the highest *RMSRE* values of 95.02% for SAE 30 and 122.31% for SAE 40. It also exhibited the highest maximum relative errors, reaching 405.19% and 537.35%, respectively. In contrast, the Koval model provided the highest predictive accuracy among the power-law models, with *RMSRE* values of approximately 3% for both oil grades and maximum relative errors below 9%. The Kendall–Monroe and Bingham models showed intermediate performance, with substantial differences in accuracy depending on the oil grade.

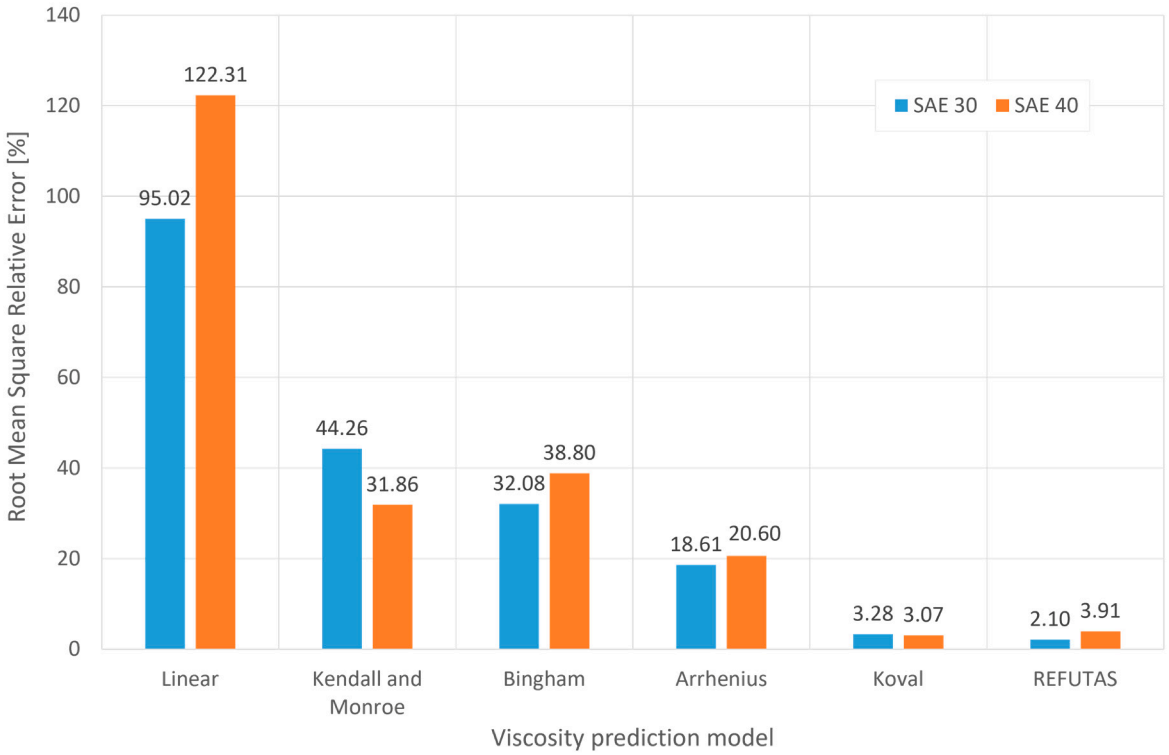


Figure 26. Root mean square relative error (RMSRE) of dynamic viscosity calculated using the investigated models for SAE 30 and SAE 40 lubricating oils.

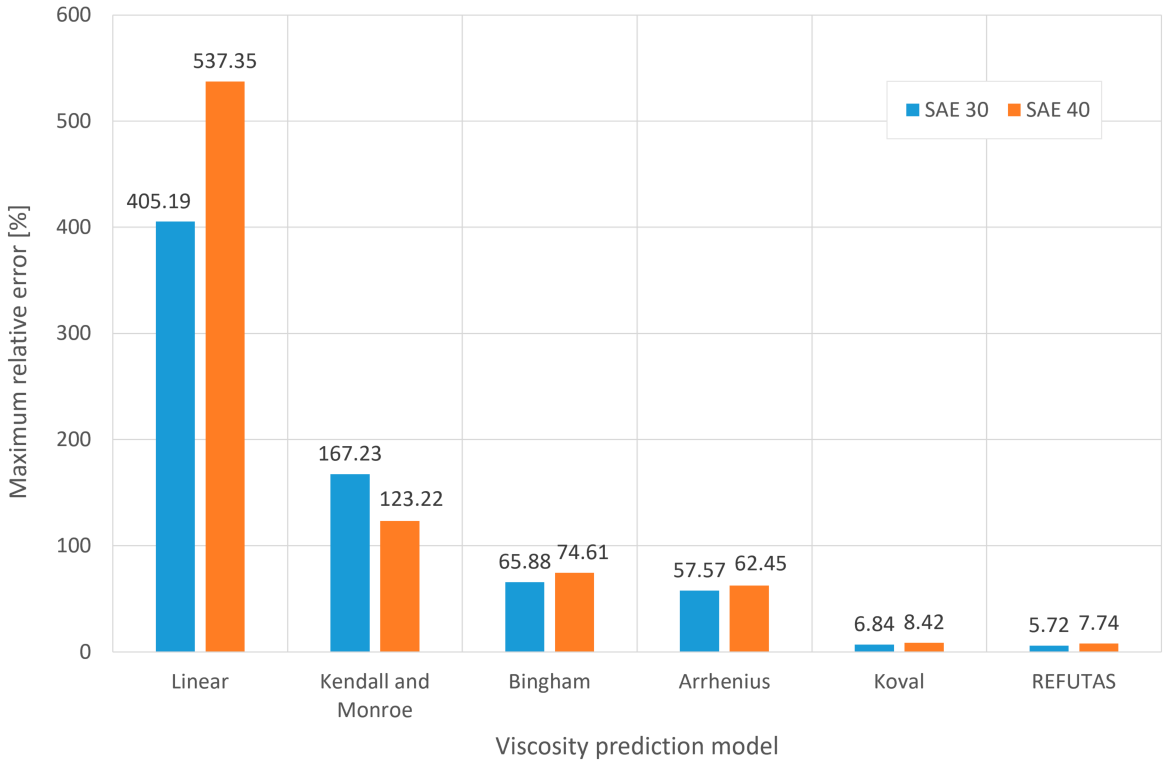


Figure 27. Maximum relative error of dynamic viscosity calculated using the investigated models for SAE 30 and SAE 40 lubricating oils.

To complement the error-based assessment, the coefficient of determination (R^2) was calculated for each investigated model. The obtained values are presented in Figure 28. The R^2 values were 0.869 and 0.843 for the linear model, 0.952 and 0.922 for the Kendall–Monroe

model, and 0.857 and 0.804 for the Bingham model for SAE 30 and SAE 40, respectively. The Arrhenius model yielded higher R^2 values of 0.988 and 0.982, whereas the Koval and REFUTAS models both reached R^2 values of 0.999 for SAE 30 and 0.997 for SAE 40. Thus, the R^2 analysis confirms the close correspondence between calculated and experimental viscosities obtained with the Koval and REFUTAS models and the substantially weaker correspondence observed for the linear and Bingham formulations.

The comparison with the non-power-law reference models is particularly noteworthy. The REFUTAS model exhibited the lowest *RMSRE* for SAE 30 (2.10%) and the lowest maximum relative error for both SAE 30 (5.72%) and SAE 40 (7.74%). The Arrhenius model provided substantially lower errors than the less accurate power-law formulations but remained clearly less accurate than Koval and REFUTAS. The R^2 values provide a consistent complementary measure of the agreement, with the highest values obtained for Koval and REFUTAS. Overall, the lowest errors were obtained for the Koval and REFUTAS models, whereas the linear model showed by far the largest deviations from the experimental data.

The parameters of the investigated models should be interpreted primarily in terms of their mathematical role in describing the viscosity of the mixture. Most of the investigated formulations are empirical or semi-empirical relationships rather than molecular or thermodynamic models. Their parameters therefore do not necessarily correspond to independent physical quantities such as activation energies or interaction parameters. Instead, they control the contribution of the component viscosities and mixture composition to the calculated viscosity and determine the degree of non-linearity of the resulting relationship. Their values are consequently dependent on the properties of the investigated components and on the temperature and composition ranges considered in the model formulation.

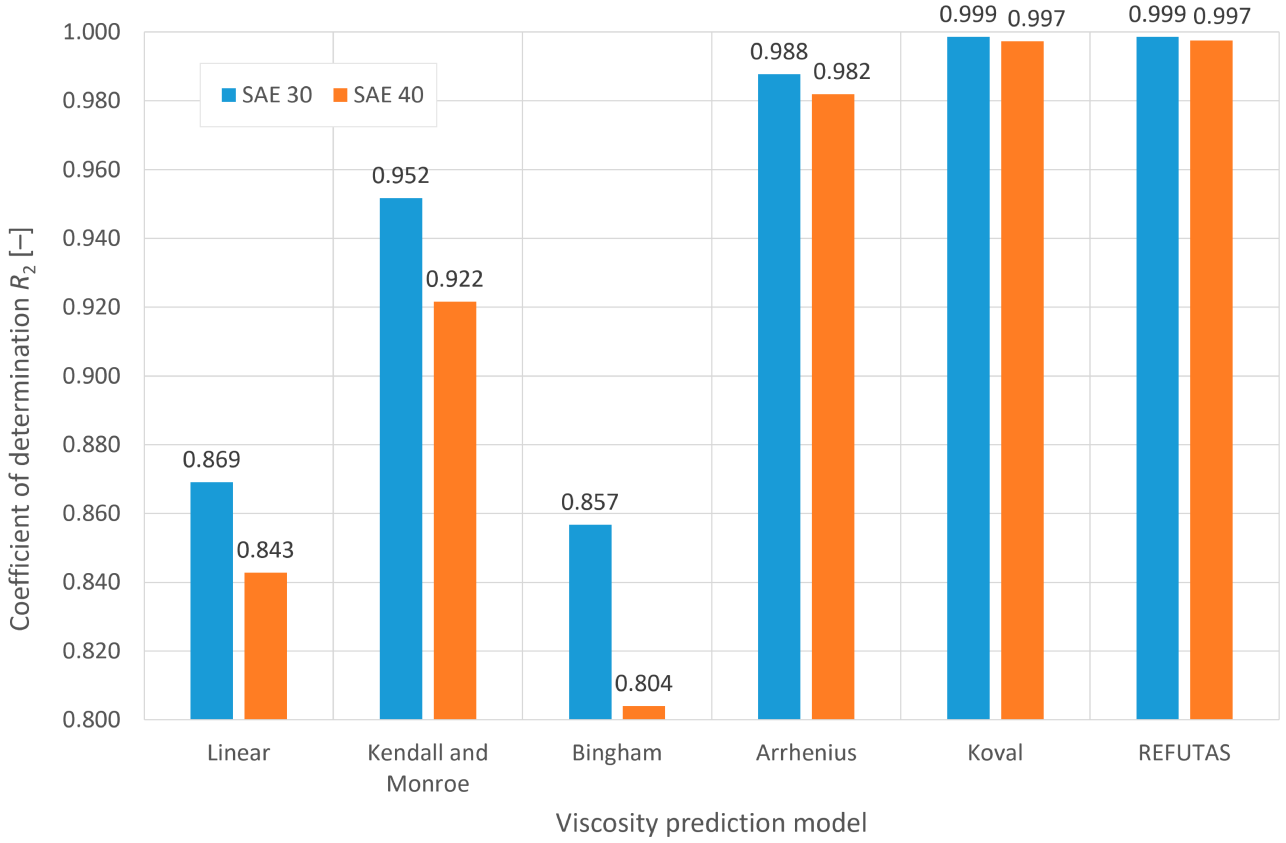


Figure 28. Coefficient of determination (R^2) between calculated and experimentally measured dynamic viscosity for the investigated models and lubricating oil grades.

The lower deviations obtained for the Koval and REFUTAS models can be explained by their greater ability to represent the non-linear dependence of mixture viscosity on diesel oil concentration. This is particularly important for the investigated systems because of the large viscosity contrast between the lubricating oil and diesel oil. The linear model assumes a constant relationship between mixture composition and viscosity and therefore cannot reproduce changes in the curvature of the experimental viscosity–composition relationship. This limitation becomes increasingly pronounced as the diesel oil concentration increases. In contrast, the mathematical forms of the Koval and REFUTAS models provide greater flexibility in describing this non-linear behaviour, which results in a closer representation of the experimental data and consequently lower deviations.

For further comparison with the empirical and semi-empirical formulations, a theoretical description of liquid viscosity can be considered using the Eyring theory of viscous flow [41]. In this approach, the dynamic viscosity is related to the free energy of activation of molecular flow, which can be expressed as

$$\eta = \frac{hN_a}{V_m} \exp\left(\frac{\Delta G‡}{RT}\right), \tag{16}$$

where h is the Planck constant, N_a is the Avogadro constant, V_m is the molar volume, $\Delta G‡$ is the Gibbs free energy of activation of viscous flow, R is the gas constant, and T is the absolute temperature.

This expression provides a physical interpretation of viscosity in terms of the molecular activation process. In contrast, the models investigated in the present study primarily establish empirical relationships between the viscosities of the components, mixture composition and temperature, without explicitly determining molecular activation parameters. Therefore, their parameters should be regarded mainly as correlation parameters, and their predictive capability should not be interpreted as a complete molecular description of the viscous flow mechanism.

The results therefore indicate that mathematical simplicity does not necessarily imply insufficient predictive capability. In the present case, the performance of a model depends not only on the number of parameters but also on whether its mathematical structure is capable of representing the non-linear dependence of viscosity on composition and temperature. This explains why the Koval model, despite its relatively simple formulation, provides substantially lower deviations than the linear model and approaches the predictive performance of the more complex REFUTAS formulation [26]. The results also demonstrate that improved empirical agreement should be interpreted as a better representation of the experimentally observed mixing behaviour rather than as direct evidence of a more complete molecular description of the viscosity of the investigated mixtures.

4. Conclusions

The results demonstrate clear differences in the predictive performance and systematic behavior of the investigated viscosity models. The comparison with experimental measurements and analysis of the relative-error distributions reveal distinct patterns of agreement and deviation for each formulation across the investigated range. The main conclusions are as follows:

1. The predictive accuracy of the investigated models depends on both mixture composition and temperature. The observed differences result primarily from the ability of each mathematical formulation to reproduce the non-linear relationship between mixture viscosity, composition and temperature.
2. The linear model provides the simplest description of the viscosity–composition relationship, but its inability to represent non-linear mixing behaviour results in

substantially larger deviations from the experimental data. In contrast, the Koval and REFUTAS models provide the lowest deviations, demonstrating that a suitable mathematical structure can provide high predictive accuracy without necessarily requiring a large number of parameters.

3. The investigated formulations are predominantly empirical or semi-empirical relationships. Their parameters primarily describe the mathematical dependence of mixture viscosity on component properties, composition and temperature and should not generally be interpreted as independent thermodynamic or molecular parameters. The Eyring theory provides a theoretical reference by relating viscosity to the Gibbs free energy of activation of viscous flow.
4. The results indicate that the suitability of power-law models for diesel oil-dilution assessment should be evaluated not only in terms of the magnitude of the error, but also its distribution over the relevant temperature and concentration ranges. The Koval model appears particularly suitable for further investigation owing to its combination of relatively simple formulation and low prediction errors.
5. From a practical perspective, the results indicate that the Koval model may offer a relatively simple formulation for applications requiring the estimation of the viscosity of lubricating oil–diesel oil mixtures. Its low prediction errors over the investigated temperature and concentration ranges suggest that it could be considered as a potential component of diagnostic procedures or lubricating oil quality monitoring systems for assessing diesel oil dilution in lubricating oils. Such an application could provide a relatively simple means of relating measured lubricating-oil viscosity to the degree of fuel contamination, subject to further validation under practical operating conditions.
6. Further work should focus on the inverse application of the most accurate power-law formulations, including the estimation of diesel oil concentration from measured lubricating-oil viscosity, propagation of viscosity measurement uncertainty into concentration uncertainty, and validation using independent mixtures and used lubricating oils obtained from operating engines.

Author Contributions: Conceptualization, L.C., M.S. (Magdalena Szmukała), I.M.-P. and M.S. (Marcin Szczepanek); methodology, L.C., I.M.-P. and M.S. (Marcin Szczepanek); validation, L.C., M.S. (Magdalena Szmukała), I.M.-P. and M.S. (Marcin Szczepanek); formal analysis, L.C., M.S. (Magdalena Szmukała), I.M.-P. and M.S. (Marcin Szczepanek); investigation, L.C., M.S. (Magdalena Szmukała), I.M.-P. and M.S. (Marcin Szczepanek); resources, L.C., M.S. (Magdalena Szmukała), I.M.-P. and M.S. (Marcin Szczepanek); data curation, L.C. and I.M.-P.; writing—original draft preparation, L.C., L.C., M.S. (Magdalena Szmukała), I.M.-P. and M.S. (Marcin Szczepanek); writing—review and editing, L.C., M.S. (Magdalena Szmukała), I.M.-P. and M.S. (Marcin Szczepanek); visualization, L.C., L.C., M.S. (Magdalena Szmukała), I.M.-P. and M.S. (Marcin Szczepanek); supervision, L.C.; project administration, L.C.; funding acquisition, L.C., I.M.-P. and M.S. (Marcin Szczepanek). All authors have read and agreed to the published version of the manuscript.

Funding: This research was funded by the statutory research funds of the Maritime University of Szczecin, grant numbers 1/S/KSO/26 and 1/S/KE/26.

Data Availability Statement: The data presented in this study are available on request from the corresponding author.

Conflicts of Interest: The authors declare no conflicts of interest.

Appendix A. Selected Physical and Rheological Properties of the Investigated Mixtures

Table A1. Density of the investigated mixtures.

SAE Viscosity Grade of the Lubricating Oil	Temperature t [°C]	Diesel Oil Content in Lubricating Oil C [% m/m]							
		0	1	2	5	10	20	50	100
		Density ρ_t [kg/m^3]							
SAE 30	40	882.65	881.59	881.32	879.25	875.89	869.48	849.88	818.44
	50	876.51	875.36	875.17	873.07	869.27	862.45	843.11	811.27
	60	870.39	869.09	868.98	866.97	863.48	856.75	836.54	804.38
	70	864.08	862.9	862.7	860.62	857.05	850.25	829.82	797.14
	80	857.94	856.67	856.41	854.37	850.83	843.82	823.46	790.04
	90	851.65	850.41	850.21	848.07	844.37	837.45	816.51	782.97
	100	845.42	844.16	843.91	841.72	838.07	830.97	809.72	775.81
SAE 40	40	883.02	882.22	881.45	879.56	875.59	869.95	850.02	818.44
	50	876.77	876.14	875.3	873.37	869.63	863.61	843.15	811.27
	60	870.58	870.13	869.12	867.29	863.52	857.51	836.82	804.38
	70	864.4	863.91	863.02	861.05	857.05	851.06	830.15	797.14
	80	858.36	857.75	856.94	854.93	850.84	844.74	823.55	790.04
	90	851.65	851.54	850.7	848.68	844.57	838.41	816.96	782.97
	100	846.04	845.45	844.58	842.43	838.35	832.13	810.31	775.81

Table A2. Kinematic viscosity of the investigated mixtures.

SAE Viscosity Grade of the Lubricating Oil	Temperature t [°C]	Diesel Oil Content in Lubricating oil C [% m/m]							
		0	1	2	5	10	20	50	100
		Kinematic Viscosity ν_t [mm^2/s]							
SAE 30	40	105.01	98.06	96.64	82.70	59.61	36.25	11.070	2.897
	50	66.11	59.28	58.72	53.89	39.73	24.97	8.461	2.443
	60	41.66	38.07	37.71	33.34	26.31	17.85	6.495	2.064
	70	28.62	26.35	26.10	23.29	18.77	13.18	5.204	1.769
	80	20.53	19.19	18.97	17.61	13.93	10.07	4.250	1.551
	90	14.99	14.30	14.16	13.29	10.67	7.916	3.545	1.376
	100	11.72	11.05	10.96	10.32	8.398	6.404	3.012	1.232
SAE 40	40	159.90	157.95	149.1	123.95	78.71	50.29	13.25	2.897
	50	98.09	92.39	87.62	73.92	50.96	34.01	10.010	2.443
	60	59.78	57.14	54.50	46.72	34.07	23.71	7.605	2.064
	70	39.91	38.44	36.73	32.01	23.91	17.15	6.040	1.769
	80	27.95	27.28	26.21	22.88	17.39	12.85	4.918	1.551
	90	20.20	19.82	19.08	16.84	13.15	9.979	4.095	1.376
	100	15.21	15.05	14.51	12.90	10.24	7.908	3.447	1.232

Table A3. Dynamic viscosity of the investigated mixtures.

SAE Viscosity Grade of the Lubricating Oil	Temperature t [°C]	Diesel Oil Content in Lubricating Oil C [% m/m]							
		0	1	2	5	10	20	50	100
		Dynamic Viscosity η_t [mPa·s]							
SAE 30	40	92.69	86.45	85.17	72.71	52.21	31.52	9.41	2.37
	50	57.95	51.89	51.39	47.05	34.54	21.54	7.13	1.98
	60	36.26	33.09	32.77	28.90	22.72	15.29	5.43	1.66
	70	24.73	22.74	22.52	20.04	16.09	11.21	4.32	1.41
	80	17.61	16.44	16.25	15.05	11.85	8.50	3.50	1.23
	90	12.77	12.16	12.04	11.27	9.01	6.63	2.89	1.08
	100	9.91	9.33	9.25	8.69	7.04	5.32	2.44	0.96

Table A3. *Cont.*

SAE Viscosity Grade of the Lubricating Oil	Temperature t [°C]	Diesel Oil Content in Lubricating Oil C [% m/m]							
		0	1	2	5	10	20	50	100
		Dynamic Viscosity η_t [mPa·s]							
SAE 40	40	141.19	139.35	131.42	109.02	68.92	43.75	11.26	2.37
	50	86.00	80.95	76.69	64.56	44.32	29.37	8.44	1.98
	60	52.04	49.72	47.37	40.52	29.42	20.33	6.36	1.66
	70	34.50	33.21	31.70	27.56	20.49	14.60	5.01	1.41
	80	23.99	23.40	22.46	19.56	14.80	10.85	4.05	1.23
	90	17.20	16.88	16.23	14.29	11.11	8.37	3.35	1.08
	100	12.87	12.72	12.25	10.87	8.58	6.58	2.79	0.96

Table A4. Density measurement uncertainties of the investigated mixtures.

SAE Viscosity Grade of the Lubricating Oil	Temperature t [°C]	Diesel Oil Content in Lubricating Oil C [% m/m]							
		0	1	2	5	10	20	50	100
		Density Measurement Uncertainty u(ρ_t) [kg/m^3]							
SAE 30	40	±0.38	±0.38	±0.38	±0.38	±0.37	±0.37	±0.37	±0.36
	50	±0.38	±0.37	±0.37	±0.37	±0.37	±0.37	±0.37	±0.36
	60	±0.37	±0.37	±0.37	±0.37	±0.37	±0.37	±0.36	±0.35
	70	±0.37	±0.37	±0.37	±0.37	±0.37	±0.37	±0.36	±0.35
	80	±0.37	±0.37	±0.37	±0.37	±0.37	±0.37	±0.36	±0.35
	90	±0.37	±0.37	±0.37	±0.37	±0.37	±0.36	±0.36	±0.35
	100	±0.37	±0.37	±0.37	±0.36	±0.36	±0.36	±0.36	±0.34
SAE 40	40	±0.38	±0.38	±0.38	±0.38	±0.37	±0.37	±0.37	±0.36
	50	±0.38	±0.37	±0.37	±0.37	±0.37	±0.37	±0.37	±0.36
	60	±0.37	±0.37	±0.37	±0.37	±0.37	±0.37	±0.36	±0.35
	70	±0.37	±0.37	±0.37	±0.37	±0.37	±0.37	±0.36	±0.35
	80	±0.37	±0.37	±0.37	±0.37	±0.37	±0.37	±0.36	±0.35
	90	±0.37	±0.37	±0.37	±0.37	±0.37	±0.36	±0.36	±0.35
	100	±0.37	±0.37	±0.37	±0.36	±0.36	±0.36	±0.36	±0.34

Table A5. Kinematic viscosity measurement uncertainties of the investigated mixtures.

SAE Viscosity Grade of the Lubricating Oil	Temperature t [°C]	Diesel Oil Content in Lubricating Oil C [% m/m]							
		0	1	2	5	10	20	50	100
		Kinematic Viscosity Measurement Uncertainty u(ν_t) [mm^2/s]							
SAE 30	40	±0.83	±0.77	±0.76	±0.66	±0.48	±0.29	±0.10	±0.03
	50	±0.54	±0.45	±0.45	±0.41	±0.29	±0.17	±0.04	±0.0404
	60	±0.27	±0.25	±0.24	±0.21	±0.17	±0.11	±0.03	±0.0002
	70	±0.18	±0.17	±0.16	±0.14	±0.11	±0.08	±0.02	±0.002
	80	±0.13	±0.12	±0.12	±0.11	±0.08	±0.06	±0.02	±0.003
	90	±0.09	±0.08	±0.08	±0.08	±0.06	±0.04	±0.01	±0.004
	100	±0.07	±0.06	±0.06	±0.06	±0.05	±0.04	±0.02	±0.01
SAE 40	40	±1.26	±1.24	±1.17	±0.98	±0.62	±0.42	±0.11	±0.03
	50	±0.77	±0.73	±0.69	±0.57	±0.39	±0.25	±0.05	±0.011
	60	±0.40	±0.38	±0.36	±0.31	±0.22	±0.15	±0.04	±0.0002
	70	±0.26	±0.25	±0.24	±0.20	±0.15	±0.10	±0.03	±0.002
	80	±0.18	±0.17	±0.16	±0.14	±0.10	±0.07	±0.02	±0.003
	90	±0.12	±0.12	±0.12	±0.10	±0.08	±0.05	±0.01	±0.004
	100	±0.09	±0.09	±0.08	±0.07	±0.06	±0.05	±0.02	±0.01

Appendix B. Dynamic Viscosity Values Calculated Using the Investigated Models

Table A6. Dynamic viscosity according to the linear model.

SAE Viscosity Grade of the Lubricating Oil	Temperature t [°C]	Diesel Oil Content in Lubricating Oil C [% m/m]							
		0	1	2	5	10	20	50	100
		Dynamic Viscosity η_t [mPa·s]							
SAE 30	40	92.69	91.78	90.88	88.17	83.66	74.62	47.53	2.37
	50	57.95	57.39	56.83	55.15	52.35	46.75	29.96	1.98
	60	36.26	35.91	35.57	34.53	32.80	29.34	18.96	1.66
	70	24.73	24.50	24.26	23.56	22.40	20.07	13.07	1.41
	80	17.61	17.45	17.29	16.79	15.97	14.34	9.42	1.23
	90	12.77	12.65	12.53	12.18	11.60	10.43	6.92	1.08
	100	9.91	9.82	9.73	9.46	9.01	8.12	5.43	0.96
SAE 40	40	141.19	139.81	138.42	134.25	127.31	113.43	71.78	2.37
	50	86.00	85.16	84.32	81.80	77.60	69.20	43.99	1.98
	60	52.04	51.54	51.04	49.52	47.00	41.97	26.85	1.66
	70	34.50	34.17	33.84	32.84	31.19	27.88	17.95	1.41
	80	23.99	23.76	23.54	22.85	21.71	19.44	12.61	1.23
	90	17.20	17.04	16.88	16.40	15.59	13.98	9.14	1.08
	100	12.87	12.75	12.63	12.27	11.68	10.49	6.91	0.96

Table A7. Dynamic viscosity based on the Kendall and Monroe model.

SAE Viscosity Grade of the Lubricating Oil	Temperature t [°C]	Diesel Oil Content in Lubricating Oil C [% m/m]							
		0	1	2	5	10	20	50	100
		Dynamic viscosity η_t [mPa·s]							
SAE 30	40	92.69	90.74	88.82	83.22	74.42	58.73	25.14	2.37
	50	57.95	56.78	55.63	52.27	46.98	37.49	16.83	1.98
	60	36.26	35.57	34.88	32.88	29.71	24.01	11.34	1.66
	70	24.73	24.28	23.83	22.52	20.44	16.68	8.21	1.41
	80	17.61	17.30	17.00	16.10	14.68	12.10	6.19	1.23
	90	12.77	12.55	12.34	11.72	10.73	8.93	4.75	1.08
	100	9.91	9.75	9.59	9.13	8.38	7.03	3.84	0.96
SAE 40	40	141.19	90.74	88.82	83.22	74.42	58.73	25.14	2.37
	50	86.00	56.78	55.63	52.27	46.98	37.49	16.83	1.98
	60	52.04	35.57	34.88	32.88	29.71	24.01	11.34	1.66
	70	34.50	24.28	23.83	22.52	20.44	16.68	8.21	1.41
	80	23.99	17.30	17.00	16.10	14.68	12.10	6.19	1.23
	90	17.20	12.55	12.34	11.72	10.73	8.93	4.75	1.08
	100	12.87	9.75	9.59	9.13	8.38	7.03	3.84	0.96

Table A8. Dynamic viscosity based on the Koval model.

SAE Viscosity Grade of the Lubricating Oil	Temperature t [°C]	Diesel Oil Content in Lubricating Oil C [% m/m]							
		0	1	2	5	10	20	50	100
		Dynamic Viscosity η_t [mPa·s]							
SAE 30	40	92.69	87.33	82.35	69.40	52.99	32.44	9.88	2.37
	50	57.95	54.97	52.19	44.83	35.22	22.62	7.58	1.98
	60	36.26	34.62	33.08	28.93	23.36	15.72	5.81	1.66
	70	24.73	23.72	22.76	20.17	16.61	11.56	4.59	1.41
	80	17.61	16.96	16.34	14.64	12.26	8.80	3.74	1.23
	90	12.77	12.34	11.93	10.80	9.19	6.79	3.07	1.08
	100	9.91	9.60	9.30	8.48	7.30	5.49	2.60	0.96

Table A8. *Cont.*

SAE Viscosity Grade of the Lubricating Oil	Temperature t [°C]	Diesel Oil Content in Lubricating Oil C [% m/m]							
		0	1	2	5	10	20	50	100
		Dynamic Viscosity η_t [mPa·s]							
SAE 40	40	141.19	131.58	122.78	100.43	73.37	41.81	11.09	2.37
	50	86.00	80.82	76.02	63.61	48.05	28.91	8.50	1.98
	60	52.04	49.29	46.72	39.96	31.18	19.80	6.49	1.66
	70	34.50	32.86	31.32	27.20	21.74	14.37	5.11	1.41
	80	23.99	22.96	21.99	19.35	15.78	10.80	4.14	1.23
	90	17.20	16.53	15.89	14.16	11.75	8.30	3.40	1.08
	100	12.87	12.41	11.97	10.76	9.06	6.57	2.85	0.96

Table A9. Dynamic viscosity based on the Bingham model.

SAE Viscosity Grade of the Lubricating Oil	Temperature t [°C]	Diesel Oil Content in Lubricating Oil C [% m/m]							
		0	1	2	5	10	20	50	100
		Dynamic Viscosity η_t [mPa·s]							
SAE 30	40	92.69	67.12	52.61	31.91	19.27	10.75	4.62	2.37
	50	57.95	45.19	37.03	24.03	15.15	8.72	3.83	1.98
	60	36.26	30.01	25.59	17.76	11.76	7.02	3.18	1.66
	70	24.73	21.22	18.58	13.54	9.32	5.74	2.67	1.41
	80	17.61	15.54	13.90	10.56	7.54	4.79	2.29	1.23
	90	12.77	11.52	10.49	8.28	6.12	4.03	1.99	1.08
	100	9.91	9.06	8.35	6.75	5.12	3.45	1.74	0.96
SAE 40	40	141.19	89.05	65.04	35.95	20.60	11.11	4.66	2.37
	50	86.00	60.40	46.54	27.57	16.41	9.07	3.87	1.98
	60	52.04	39.93	32.39	20.67	12.90	7.36	3.22	1.66
	70	34.50	27.94	23.48	15.87	10.31	6.06	2.71	1.41
	80	23.99	20.23	17.49	12.44	8.39	5.09	2.33	1.23
	90	17.20	14.96	13.24	9.84	6.89	4.31	2.03	1.08
	100	12.87	11.44	10.30	7.93	5.73	3.68	1.78	0.96

Table A10. Dynamic viscosity based on the Arrhenius model.

SAE Viscosity Grade of the Lubricating Oil	Temperature t [°C]	Diesel Oil Content in Lubricating Oil C [% m/m]							
		0	1	2	5	10	20	50	100
		Dynamic Viscosity η_t [mPa·s]							
SAE 30	40	92.69	89.35	86.13	77.16	64.24	44.52	14.82	2.37
	50	57.95	56.02	54.16	48.95	41.35	29.50	10.72	1.98
	60	36.26	35.16	34.09	31.08	26.64	19.57	7.76	1.66
	70	24.73	24.03	23.35	21.43	18.57	13.95	5.91	1.41
	80	17.61	17.15	16.70	15.42	13.49	10.34	4.65	1.23
	90	12.77	12.45	12.15	11.28	9.97	7.79	3.71	1.08
	100	9.91	9.68	9.46	8.81	7.84	6.21	3.08	0.96
SAE 40	40	141.19	135.54	130.11	115.10	93.83	62.35	18.30	2.37
	50	86.00	82.82	79.76	71.23	58.99	40.46	13.06	1.98
	60	52.04	50.28	48.58	43.81	36.88	26.13	9.30	1.66
	70	34.50	33.41	32.36	29.40	25.06	18.20	6.97	1.41
	80	23.99	23.29	22.61	20.68	17.82	13.23	5.42	1.23
	90	17.20	16.73	16.28	14.98	13.04	9.88	4.31	1.08
	100	12.87	12.54	12.22	11.30	9.92	7.65	3.51	0.96

Table A11. Dynamic viscosity based on the REFUTAS model.

SAE Viscosity Grade of the Lubricating Oil	Temperature t [°C]	Diesel Oil Content in Lubricating Oil C [% m/m]							
		0	1	2	5	10	20	50	100
		Dynamic Viscosity η_t [mPa·s]							
SAE 30	40	92.69	87.24	82.25	69.11	52.42	31.61	9.36	2.37
	50	57.95	54.84	51.98	44.38	34.49	21.74	7.12	1.98
	60	36.26	34.50	32.89	28.53	22.75	15.00	5.43	1.66
	70	24.73	23.63	22.62	19.85	16.13	11.00	4.29	1.41
	80	17.61	16.89	16.23	14.40	11.90	8.36	3.49	1.23
	90	12.77	12.29	11.85	10.63	8.93	6.46	2.88	1.08
	100	9.91	9.56	9.24	8.35	7.09	5.23	2.44	0.96
SAE 40	40	141.19	131.68	122.93	100.58	73.15	41.10	10.51	2.37
	50	86.00	80.72	75.80	63.13	47.21	27.86	7.95	1.98
	60	52.04	49.17	46.46	39.41	30.34	18.85	6.02	1.66
	70	34.50	32.75	31.10	26.75	21.03	13.59	4.72	1.41
	80	23.99	22.87	21.82	19.00	15.24	10.19	3.82	1.23
	90	17.20	16.48	15.78	13.90	11.35	7.84	3.15	1.08
	100	12.87	12.36	11.87	10.56	8.75	6.21	2.65	0.96

References

1. Kaminski, P. Investigation Lubricity Performance of Lubricating Oil Used in Marine Diesel Engine—Fuel Injection Pump. *Appl. Sci.* **2024**, *14*, 6148. [CrossRef]
2. Taylor, R.I. Fuel-Lubricant Interactions: Critical Review of Recent Work. *Lubricants* **2021**, *9*, 92. [CrossRef]
3. Babu, S.S.; Nadge, P.; Sen, S. Experimental Investigation and Prediction of Viscosity and Contamination Percentage of Fuel Dilution in Oil as a Function of Temperature for Turbo Machinery. *Int. J. Adv. Eng. Manag.* **2021**, *3*, 443–449.
4. Ito, T.; Kitamura, T.; Kojima, H.; Kawanabe, H. Prediction of Oil Dilution by Post-Injection in DPF Regeneration Mode. In Proceedings of the 2019 JSAE/SAE Powertrains, Fuels and Lubricants, Kyoto, Japan, 26 August 2019. [CrossRef]
5. Fluid Life Why Diesel Fuel Dilution Is Bad for Your Engine. Available online: https://www.fluidlife.com/resource-center/data-interpretation/documents/diesel-fuel-dilution-bad-for-engine/?srsltid=AfmBOorfPD3AOOoWYoDWM3V06Hy5frcJUN3GBanqXVAg2ds843GZd9bG (accessed on 29 July 2026).
6. Altman, L.J.; Reischman, P.T. Method for Detecting Fuel Dilution of Marine Lubricating Oils. U.S. Patent 5,169,785, 26 October 1990.
7. Yu, M.; Zhang, J.; Joedicke, A.; Reddyhoff, T. Experimental Investigation into the Effects of Diesel Dilution on Engine Lubrication. *Tribol. Int.* **2021**, *156*, 106828. [CrossRef]
8. Niedermayer, A.O.; Voglhuber-Brunnmaier, T.; Heinisch, M.; Feichtinger, F.; Jakoby, B. Monitoring of the Dilution of Motor Oil with Diesel Using an Advanced Resonant Sensor System. *Procedia Eng.* **2016**, *168*, 15–18. [CrossRef]
9. MAHLE Aftermarket Inc. *Engine Components and Filters: Damage Profiles, Probable Causes and Prevention*; mahled-317; MAHLE Aftermarket Inc.: Farmington Hills, MI, USA, 2010.
10. Ragupathi, K.; Mani, I. Durability and Lube Oil Contamination Study on Diesel Engine Fueled with Various Alternative Fuels: A Review. *Energy Sources Part A Recovery Util. Environ. Eff.* **2021**, *43*, 932–943. [CrossRef]
11. Shanta, S.M.; Molina, G.J.; Soloiu, V. Tribological Effects of Mineral-Oil Lubricant Contamination with Biofuels: A Pin-on-Disk Tribometry and Wear Study. *Adv. Tribol.* **2011**, *2011*, 820795. [CrossRef]
12. Chybowski, L.; Szczepanek, M.; Sztangierski, R.; Brożek, P. A Quantitative and Qualitative Analysis of the Lubricity of Used Lubricating Oil Diluted with Diesel Oil. *Appl. Sci.* **2024**, *14*, 4567. [CrossRef]
13. Skonieczna, D.; Vrublevskyi, O.; Janulin, M.; Szczyglak, P. Analysis of Tribological Properties of Engine Lubricants Used in Hybrid Vehicles. *Materials* **2024**, *17*, 5304. [CrossRef] [PubMed]
14. DFC Diesel. Failure Analysis. Available online: https://dfcdiesel.com/warranty-info/failure-analysis/ (accessed on 16 June 2026).
15. Kamiński, W.; Michalska-Pożoga, I. Possibility of Marine Low-Speed Engine Piston Ring Wear Prediction during Real Operational Conditions. *Energies* **2023**, *16*, 1433. [CrossRef]
16. Ramírez-de-Santiago, M. Viscosity of Binary Liquid Mixtures: A Comparative Analysis of Mixing Rules. *Ind. Eng. Chem. Res.* **2024**, *63*, 22470–22480. [CrossRef]
17. Bingham, E.C. The Viscosity of Binary Mixtures. *J. Phys. Chem.* **1914**, *18*, 157–165. [CrossRef]

18. Prabhune, A.; Mathur, A.; Saha, S.; Dey, R. Predictive, Correlative and Machine Learning Models for Estimation of Viscosity of Liquid Mixtures. *J. Mol. Liq.* **2024**, *397*, 124147. [CrossRef]
19. Koval, E.J. A Method for Predicting the Performance of Unstable Miscible Displacement in Heterogeneous Media. *Soc. Pet. Eng. J.* **1963**, *3*, 145–154. [CrossRef]
20. Bingham, E. *The Conductivity and Viscosity of Solutions of Certain Salts in Mixtures of Acetone with Methyl Alcohol, with Ethyl Alcohol and Water*; Johns Hopkins University: Baltimore, MD, USA, 1905.
21. Hernández, E.A.; Sánchez-Reyna, G.; Ancheyta, J. Evaluation of Mixing Rules to Predict Viscosity of Petrodiesel and Biodiesel Blends. *Fuel* **2021**, *283*, 118941. [CrossRef]
22. Kamiński, W. Study to Develop Prediction Models to Determine the Most Suitable Cylinder Lubricating Oil Feed Rates for Marine Slow-Speed Engines Running on Low Sulphur Fuel Oil. *Measurement* **2025**, *247*, 116838. [CrossRef]
23. Arrhenius, S. Über Die Innere Reibung Verdünnter Wässeriger Lösungen. *Z. Phys. Chem.* **1887**, *1*, 285–298. [CrossRef]
24. British Petroleum Co. *Sunbury Report No. 3282*; British Petroleum Co.: Sunbury-on-Thames, UK, 1947.
25. British Petroleum Co. *Sunbury Report No. 3339*; British Petroleum Co.: Sunbury-on-Thames, UK, 1947.
26. Chybowski, L.; Szczepanek, M.; Kowalak, P. SATUFER Method for Determining the Degree of Lubricating Oil Dilution with Diesel Oil in an Internal Combustion Engine Lubrication System. *Energies* **2026**, *19*, 1833. [CrossRef]
27. Chybowski, L.; Szczepanek, M.; Gawdzińska, K. Arrhenius Equation for Calculating Viscosity in Assessing the Dilution Level of Lubricating Oil with Diesel Oil—A Case Study of SAE 30 and SAE 40 Grade Marine Lubricating Oils. *Energies* **2024**, *17*, 444. [CrossRef]
28. Chybowski, L.; Dąbrowski, P.; Kowalak, P.; Ćwirko, K.; Szczepanek, M. Improving the Accuracy of a New Viscosity-Based Method for Estimating Lubricating Oil Dilution by Diesel Oil in an Internal Combustion Engine. *Sci. J. Marit. Univ. Szczec.* **2026**, *86*, 44–53. [CrossRef] [PubMed]
29. ORLEN S.A. *Diesel: Ekodiesel ULTRA B, D, F, Class 2; EFECTA DIESEL B, D, F; VERVA ON B, D, F. Safety Data Sheet*; ORLEN S.A.: Płock, Poland, 2026.
30. *ZN-ORLEN-5:2019*; Przetwory Naftowe—Olej Napędowy EFECTA DIESEL. Polski Koncern Naftowy ORLEN Spółka Akcyjna: Płock, Poland, 2019.
31. *ISO 8217:2024*; Petroleum Products—Fuels (Class F)—Specifications of Marine Fuels. 7th ed. ISO: Geneva, Switzerland, 2024.
32. *PN-EN ISO 12185:2024-08*; Crude Petroleum, Petroleum Products and Related Products—Determination of Density—Laboratory Density Meter with an Oscillating U-Tube Sensor. Polish Committee for Standardization: Warsow, Poland, 2024.
33. *PN EN ISO 3104:2024-01*; Petroleum Products—Transparent and Opaque Liquids—Determination of Kinematic Viscosity and Calculation of Dynamic Viscosity. ISO: Geneva, Switzerland, 2024.
34. *ASTM D2270*; Viscosity Index (VI) from 40 °C and 100 °C. Anton Paar: Graz, Austria, 2025.
35. Eni S.p.A., Refining & Marketing. *Eni CLADIUM 120 SAE 30*; Eni S.p.A., Refining & Marketing: Rome, Italy, 2018.
36. Alvesta Kokoszyński Garncarz S.C. *AGIP Cladium 120 SAE 40 CD*; Alvesta Kokoszyński Garncarz S.C.: Szczecin, Poland, 2018.
37. Chybowski, L. *Rozcieńczenie Oleju Paliwem Jako Czynnik Ryzyka Eksplozji w Skrzyniach Korbowych Okrętowych Bezwodzikowych Silników Spalinowych*; Maritime University of Szczecin Press: Szczecin, Poland, 2023; ISBN 978-83-64434-56-3.
38. *JCGM 100:2008*; Evaluation of Measurement Data—Guide to the Expression of Uncertainty in Measurement (GUM 1995 with Minor Corrections). Joint Committee for Guides in Metrology: Sèvres, France, 2008.
39. Chybowski, L.; Kowalak, P.; Szczepanek, M.; Jóźwiak, P.; Danisiewicz, P. The Assessment of Surface Acoustic Wave Sensing for Testing Fuel Dilution of Lubricating Oils. *Measurement* **2024**, *231*, 114589. [CrossRef]
40. *ASTM D445-24*; Standard Test Method for Kinematic Viscosity of Transparent and Opaque Liquids (and Calculation of Dynamic Viscosity). ASTM International: West Conshohocken, PA, USA, 2024.
41. Eyring, H. Viscosity, Plasticity, and Diffusion as Examples of Absolute Reaction Rates. *J. Chem. Phys.* **1936**, *4*, 283–291. [CrossRef]

Disclaimer/Publisher's Note: The statements, opinions and data contained in all publications are solely those of the individual author(s) and contributor(s) and not of MDPI and/or the editor(s). MDPI and/or the editor(s) disclaim responsibility for any injury to people or property resulting from any ideas, methods, instructions or products referred to in the content.